

Chiral Aromatase and Dual Aromatase–Steroid Sulfatase Inhibitors from the Letrozole Template: Synthesis, Absolute Configuration, and In Vitro Activity[†]

Paul M. Wood,[‡] L. W. Lawrence Woo,[‡] Jean-Robert Labrosse,[‡] Melanie N. Trusselle,^{‡,†} Sergio Abbate,[§] Giovanna Longhi,[§] Ettore Castiglioni,^{§,||} France Lebon,[§] Atul Purohit,[⊥] Michael J. Reed,[⊥] and Barry V. L. Potter^{*,‡}

Medicinal Chemistry, Department of Pharmacy and Pharmacology and Sterix Ltd., University of Bath, Claverton Down, Bath, BA2 7AY, United Kingdom, Dipartimento di Scienze Biomediche e Biotecnologie, Università di Brescia, Viale Europa 11, 25133 Brescia, Italy, JASCO Corporation, 2967-5 Ishikawa-cho, Hachioji-shi, Tokyo, Japan, Endocrinology and Metabolic Medicine and Sterix Ltd., Imperial College London, Faculty of Medicine, St. Mary's Hospital, London, W2 1NY, United Kingdom

Received February 18, 2008

To explore aromatase inhibition and to broaden the structural diversity of dual aromatase–sulfatase inhibitors (DASIs), we introduced the steroid sulfatase (STS) inhibitory pharmacophore to letrozole. Letrozole derivatives were prepared bearing bis-sulfamates or mono-sulfamates with or without adjacent substituents. The most potent of the achiral and racemic aromatase inhibitor was **40** (IC₅₀ = 3.0 nM). Its phenolic precursor **39** was separated by chiral HPLC, and the absolute configuration of each enantiomer was determined using vibrational and electronic circular dichroism in tandem with calculations of the predicted spectra. Of the two enantiomers, (*R*)-phenol (**39a**) was the most potent aromatase inhibitor (IC₅₀ = 0.6 nM, comparable to letrozole), whereas the (*S*)-sulfamate, (**40b**) inhibited STS most potently (IC₅₀ = 553 nM). These results suggest that a new structural class of DASI for potential treatment of hormone-dependent breast cancer has been identified, and this is the first report of STS inhibition by an enantiopure nonsteroidal compound.

Introduction

The position of tamoxifen as the standard adjuvant treatment for hormone-dependent breast cancer (HDBC)^a in postmenopausal women is now being challenged by the third generation of aromatase inhibitors (AIs), which comprises the nonsteroidal compounds anastrozole and letrozole and the steroidal exemestane (Figure 1).^{1–4} This modification of the treatment paradigm has arisen from the results of a number of large randomized neoadjuvant and adjuvant clinical trials in which the AIs have been shown to exhibit an improved efficacy compared to tamoxifen.^{5–8} Of the third generation AIs, letrozole is 2–5 times more potent than both anastrozole and exemestane in noncellular systems and 10–20 times more potent in cellular systems.⁹ At present it is unclear whether these differences in potency will be meaningful in the clinic; however, the Femara versus Anastrozole clinical evaluation (FACE) trial is seeking to address this issue in the adjuvant setting.¹⁰

Whereas tamoxifen antagonizes the binding of estrogens to the estrogen receptor in a breast tumor, AIs inhibit the cytochrome P450 enzyme aromatase, which is responsible for the final step in the conversion of androgens to estrogens, resulting in a reduction in circulating estrogen levels. Exemes-

tane is a mechanism-based or suicide inhibitor, which is metabolized to a reactive species that irreversibly binds to the enzyme active site causing enzyme inactivation. In contrast, letrozole and anastrozole are reversible inhibitors, whose mechanism of action involves coordination to the heme iron of aromatase by one of the *N* atoms contained within the triazole moiety.

While the potential application of AIs has broadened, a new strategy for estrogen deprivation has arisen from the development of inhibitors of the enzyme steroid sulfatase (STS). STS is responsible for the hydrolysis of alkyl and aryl steroid sulfates to their unconjugated and biologically active forms. In breast cancer tissue, it has been shown that 10 times more estrone originates from estrone sulfate than from androstenedione.¹¹ In addition, STS controls the formation of dehydroepiandrosterone (DHEA) from DHEA-sulfate (DHEA-S). DHEA can be subsequently converted to androst-5-ene-3 β ,17 β -diol, an androgen with estrogenic properties capable of stimulating the growth of breast cancer cells in vitro¹² and supports the growth of carcinogen induced mammary tumors in rodents.¹³ A number of steroidal and nonsteroidal irreversible STS inhibitors have been developed,^{14–16} and the nonsteroidal compound STX64 (BN83495, Figure 1)^{17–19} has been evaluated in a phase I clinical trial for the treatment of patients with advanced breast cancer.²⁰ In this trial, stable disease was observed in 5 out of 8 evaluable patients receiving a treatment protocol consisting of either a 5 or a 20 mg daily dose of STX64.

The development of a dual aromatase–sulfatase inhibitor (DASI) is an attractive concept as this single agent should inhibit estrogen synthesis by both the aromatase and STS pathway and additionally inhibit the formation of DHEA from DHEA-S. The synthesis and biological activity of the first series of DASIs based on the known AI YM511 (4-((4-bromobenzyl)(4*H*-1,2,4-triazol-4-yl)amino)benzotrile) have been previously reported by us (**1**, Figure 2).^{21,22} Furthermore, we have recently reported on the synthesis and in vitro and in vivo inhibitory activity of novel compounds based upon the letrozole and anastrozole templates.^{23,24} In addition to

[†] This paper is dedicated to Dr. Melanie Trusselle (1973–2008).

* To whom correspondence should be addressed. Phone: +44 1225 386639. Fax: +44 1225 386114. E-mail: B.V.L.Potter@bath.ac.uk.

[‡] Department of Pharmacy and Pharmacology and Sterix Ltd., University of Bath.

[§] Dipartimento di Scienze Biomediche e Biotecnologie, Università di Brescia.

^{||} JASCO Corporation, Tokyo.

[⊥] Endocrinology and Metabolic Medicine and Sterix Ltd., Imperial College London.

^a Abbreviations: AC, Absolute configuration; AIs, aromatase inhibitors; DASI, dual aromatase–sulfatase inhibitor; DFT, density functional theory; DHEA, dehydroepiandrosterone; DHEA-S, dehydroepiandrosterone sulfate; ECD, electronic circular dichroism; FACE, femara versus anastrozole clinical evaluation; HDBC, hormone-dependent breast cancer; STS, steroid sulfatase; TDDFT, time dependent density functional theory; VCD, vibrational circular dichroism.

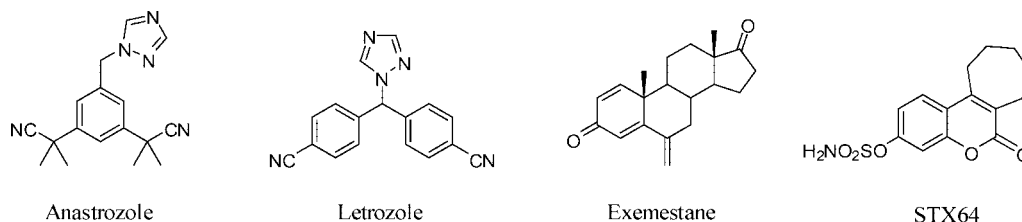


Figure 1. Third generation aromatase inhibitors anastrozole, letrozole, and exemestane and steroid sulfatase inhibitor STX64.

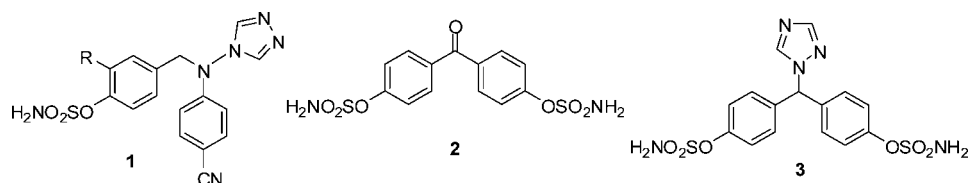
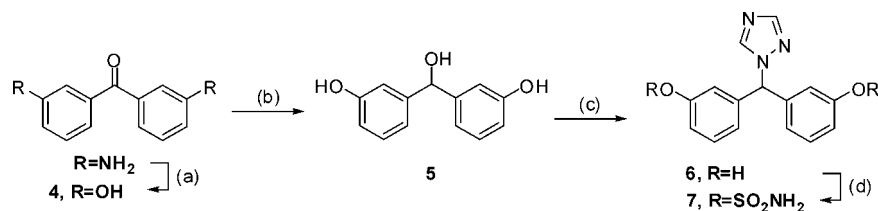


Figure 2. A YM511-based DASI **1**, 4,4'-benzophenone bis-sulfamate **2** and prototype DASI **3**.

Scheme 1. Synthesis of **7**^a



^a Reagents and conditions: (a) NaNO₂, conc H₂SO₄, 85% H₃PO₄, 0 °C; (b) NaBH₄, EtOH/H₂O, r.t.; (c) 1,2,4-triazole, *p*-toluenesulfonic acid (*p*-TSA), toluene, reflux; (d) H₂NSO₂Cl, DMA, r.t.

our nonsteroidal DASIs, there has been interest in a steroidal DASI, with Numazawa et al.²⁵ reporting the conversion of a series of steroidal AIs²⁶ to give a range of STS inhibitors based on estrogen-3-sulfamates. The sulfamates were good to potent STS inhibitors (best IC₅₀ STS = 15 nM) but were found to be weak AIs (best IC₅₀ AROM = 41.8 μM).

In the design of the first letrozole-based DASI, dual aromatase and sulfatase inhibition was achieved by replacing both of the *para*-cyano groups in letrozole with sulfamates while retaining both the triazole and the diphenylmethane moieties necessary for aromatase inhibition. Evidence supporting the design of an STS inhibitor based on this template was provided by the benzophenone-based series of STS inhibitors. In this series of compounds, a bis-sulfamate was found to be a more potent STS inhibitor than its corresponding mono-sulfamate,^{27,28} with IC₅₀ values of 0.19 and 5.1 μM for 4,4'-benzophenone bis-sulfamate (**2**, Figure 2) and its 4-mono-sulfamate congener against recombinant human STS.²⁸ This design process resulted in the synthesis of the prototype DASI, bis-sulfamate **3**, which exhibited IC₅₀ values of 3044 nM for aromatase and >10 μM for STS in JEG-3 cells. However, at a single oral dose of 10 mg/kg, **3** inhibited aromatase and rat liver STS by 60% and 88% respectively 24 h after administration.²³

The objective of this current work was to investigate the structure–activity relationship (SAR) of letrozole derived DASIs. We report the effects on activity of relocating the sulfamate groups to the *meta*-positions and the synthesis of the first chiral DASI candidates, in which one of the *para*-cyano groups of letrozole was replaced by a sulfamate group, as well as the assignment of absolute configuration using chiroptical techniques.

Results and Discussion

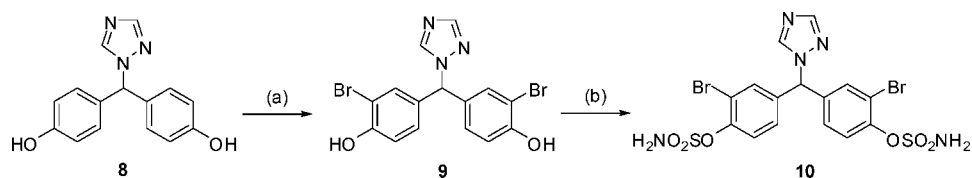
Chemistry. The reference AI, letrozole, was prepared by the alkylation of 1,2,4-triazole with α-bromomethyl-*p*-tolunitrile

followed by reaction with 4-fluorobenzonitrile according to the procedure described by Bowman et al.^{23,29} The reference STS inhibitor STX64 was synthesized according to the method of Woo et al.¹⁷

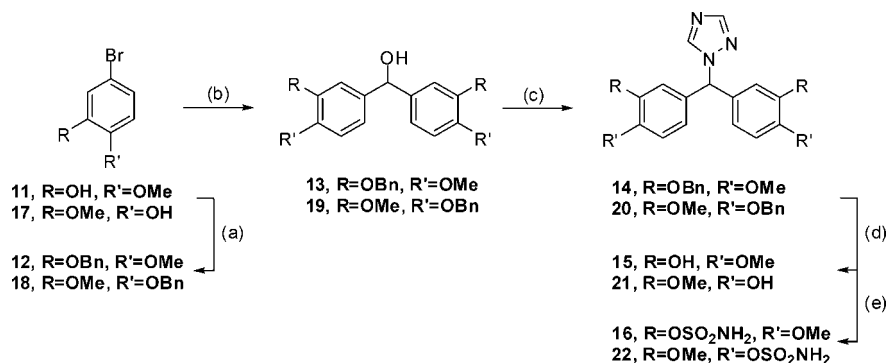
All of the novel sulfamates and phenols described in this paper were prepared according to the schemes 1–4. The final compounds and intermediates were characterized by standard analytical methods and, in addition to this, the purity of the compounds tested *in vitro* was evaluated using HPLC and they were >99% pure.

The first two compounds (**3** and **7**) synthesized differ from letrozole by having no cyano groups but instead sulfamate groups at either the *para* or *meta* positions on the aromatic ring. We previously reported the synthesis of **3** from the commercially available 4,4'-dihydroxybenzophenone.²³ The synthesis of **7** commences with the formation of 3,3'-dihydroxybenzophenone **4** from 3,3'-diaminobenzophenone according to the method of Wittig via diazotization followed by hydroxy-dediazotiation (Scheme 1).³⁰ Hejaz et al.²⁷ previously reported the synthesis of the starting 3,3'-dihydroxybenzophenone, albeit via a longer route, from the nitration of benzophenone followed by reduction, diazotization, and hydroxy-dediazotiation reactions. The reduction of ketone **4** with NaBH₄ gave **5**, from which the hydroxyl group could be displaced with 1,2,4-triazole in refluxing toluene to provide **6**. This bis-phenol was converted to 3,3'-bis-sulfamate **7** with an excess of sulfamoyl chloride in *N,N*-dimethylacetamide (DMA) according to the conditions described by Okada et al.³¹

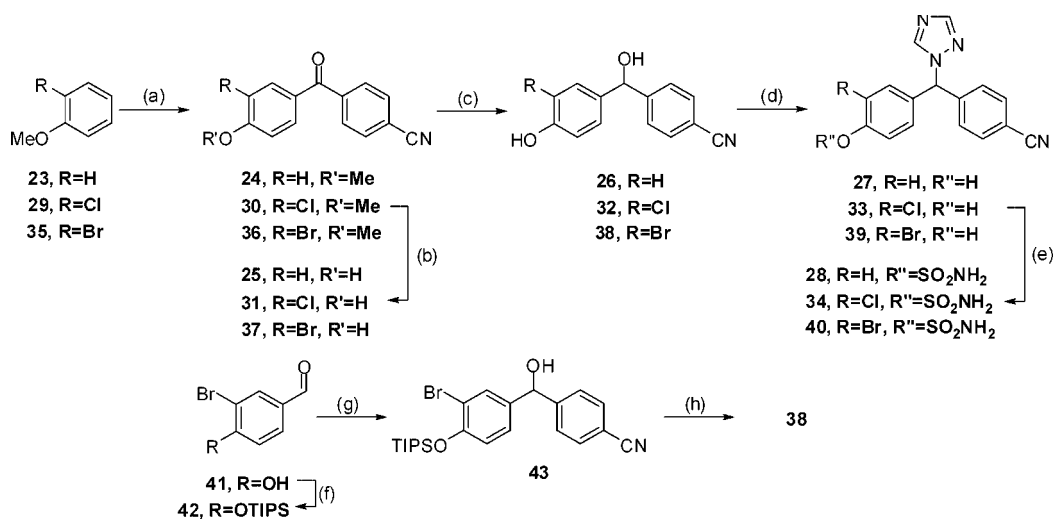
A variety of different reagents were investigated for the synthesis of dibromo derivative **10** from the corresponding bis-phenol (**8**, Scheme 2). Treatment of **8** with bromine in either acetic acid or carbon tetrachloride gave complex mixtures comprising of tetrabromo-, tribromo-, dibromo-, and monobromo- compounds with the tetrabromo- derivative predominating. The reaction of **8** with bromine in tetrahydrofuran (THF)

Scheme 2. Synthesis of **10**^a

^a Reagents and conditions: (a) $C_6H_5CH_2N(CH_3)_3Br_3$, DCM/MeOH, $-78\text{ }^\circ\text{C}$ to r.t.; (b) H_2NSO_2Cl , DMA, r.t.

Scheme 3. Synthetic Routes to **16** and **22**^a

^a Reagents and conditions: (a) NaH, BnBr, DMF, r.t.; (b) *n*-BuLi, 3-benzyloxy-4-methoxybenzaldehyde with **12** or 4-benzyloxy-3-methoxybenzaldehyde with **18**, THF, $-78\text{ }^\circ\text{C}$ to r.t.; (c) 1,2,4-triazole, *p*-TSA, toluene, reflux; (d) H_2 , Pd/C (10%), THF/MeOH, r.t.; (e) H_2NSO_2Cl , DMA, r.t.

Scheme 4. Synthetic Routes to **28**, **34**, and **40**^a

^a Reagents and conditions: (a) 4-cyanobenzoyl chloride, $AlCl_3$, r.t.; (b) pyridine hydrochloride, $220\text{ }^\circ\text{C}$ with **24** and **30** or BBr_3 , DCM, r.t. with **36**; (c) $NaBH_4$, EtOH/ H_2O , r.t.; (d) 1,2,4-triazole, *p*-TSA, toluene, reflux; (e) H_2NSO_2Cl , DMA, r.t.; (f) triisopropylsilyl chloride, imidazole, DMF, r.t.; (g) (4-cyanophenyl)magnesium chloride, THF, $0\text{ }^\circ\text{C}$ to r.t.; (h) TBAF, THF, r.t.

and sodium bicarbonate at $-78\text{ }^\circ\text{C}$ produced a mixture of starting material and the monobromo derivative. More promising results were obtained when either benzyl trimethylammonium tribromide or tetrabutylammonium tribromide was used, with the reagent of choice being the former. At $-78\text{ }^\circ\text{C}$ in dichloromethane (DCM)/MeOH, this reagent gave **9** in good yield (72%). Subsequent sulfamoylation of the bis-phenol in the usual manner furnished the desired dibromo-bis-sulfamate **10**.

The syntheses of the two methoxy group-containing sulfamates **16** and **22** are outlined in Scheme 3. For **16**, the synthesis commences with the preparation of 5-bromo-2-methoxyphenol **11** from 5-bromo-2-methoxybenzaldehyde by Baeyer–Villiger oxidation followed by hydrolysis according to the method of Van der Mey et al.³² The resulting phenol was subsequently benzyl protected to give **12** from which the methoxyphenyl-

lithium salt was generated in situ and reacted with 3-benzyloxy-4-methoxybenzaldehyde to give benzhydrol **13**. From this intermediate, the preparation of **16** was achieved using the methodology described above via reaction with triazole, deprotection and sulfamoylation. Compound **22** was synthesized analogously from the commercially available 4-bromoguaiacol **17** and 4-benzyloxy-3-methoxybenzaldehyde (Scheme 3).

The initial synthetic pathways for the three mono-sulfamates **28**, **34**, and **40** are shown in Scheme 4. For the preparation of **28**, the first step is the synthesis of **24** from anisole **23** and 4-cyanobenzoyl chloride according to the method of Leigh et al.³³ Both chloro- and bromo-substituted benzophenones **30** and **36** were prepared in an analogous fashion from 2-chloroanisole **29** and 2-bromoanisole **35** (a small amount of **24** was also obtained from this reaction), respectively. The demethylation

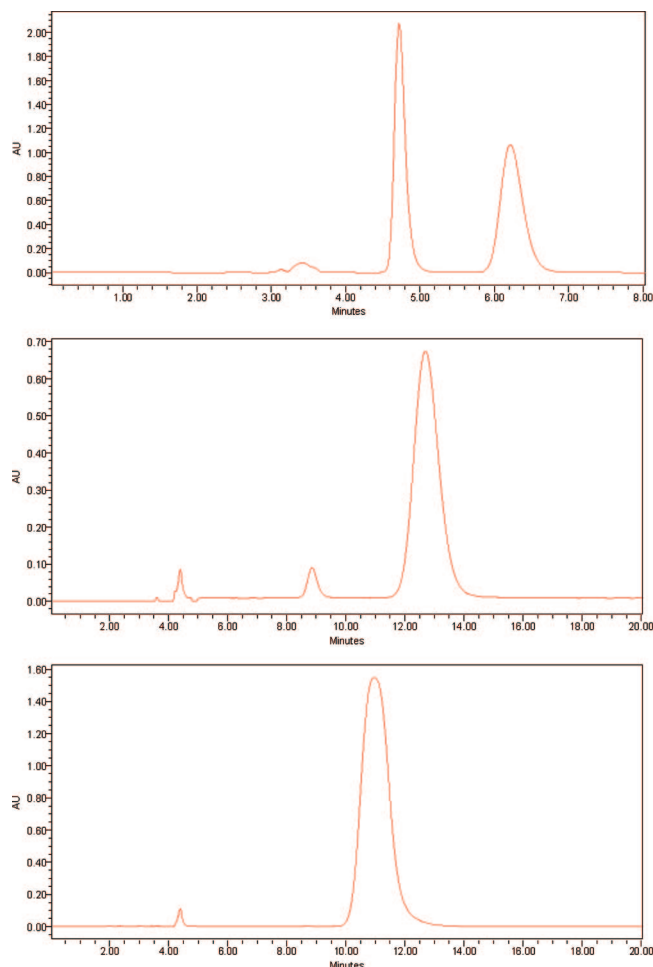


Figure 3. Top trace: Separation of racemic **39** with a Chiralpak AD-H column (250 mm \times 4.6 mm, 5 μ m). Mobile phase: MeOH; flow rate: 1.0 mL/min; detection UV: 230 nm; temperature: 25 $^{\circ}$ C; t_1 4.76 min (**39a**), t_2 6.23 min (**39b**). Middle trace: HPLC trace of **40a** (A, t_r 12.69 min) obtained with a Chiralpak AD-H column (250 mm \times 4.6 mm, 5 μ m). Mobile phase: 85% MeOH/H₂O; flow rate: 0.8 mL/min; PDA detector; temperature: 25 $^{\circ}$ C. Bottom trace: HPLC trace of **40b** (B, t_r 10.96 min) details as for **40a**.

of **24** and **30** to their corresponding phenols **25** and **31** was achieved by heating at 220 $^{\circ}$ C with pyridine hydrochloride. This method was unsuitable for the demethylation of **36**, as it produced a mixture of the three phenols **25**, **31**, and **37**, which could not be easily separated. Demethylation of **36** was achieved by treatment with BBr₃ in DCM which gave **37** as the sole phenolic product, albeit at the expense of extended reaction times. The three benzophenones **25**, **31**, and **37** were successfully reduced with NaBH₄ to give secondary alcohols **26**, **32**, and **38**, respectively, which were converted to sulfamates **28**, **34**, and **40** using the methodology described above.

The problematic demethylation step encountered in the synthesis of **40**, as well as the larger quantity required for various studies, was the driving force for the development of a modification to the synthesis, and this is outlined in Scheme 4. The commercially available 3-bromo-4-hydroxybenzaldehyde was triisopropylsilyl protected and reacted with (4-cyanophenyl)magnesium chloride³⁴ (generated by halogen metal exchange between 4-iodobenzonitrile and isopropylmagnesium chloride) to give **43**, which was subsequently deprotected with tetra-*n*-butylammonium fluoride (TBAF) to give **38** as above. This

modified route provides a faster and cleaner method for the synthesis of **40** and could also be applied for the synthesis of **28** and **34**.

Chiral HPLC. The three monosulfamates in this series were initially evaluated as racemic mixtures; to explore the full SAR of interactions with target proteins, it later became desirable to ascertain the individual activities of each enantiomer of the most potent compound. To avoid any possible complications arising from the potential decomposition of the sulfamate, the resolution was undertaken with the parent phenol, which could later be converted to the sulfamate. Attempts to separate the enantiomers of **39** by the preparation of diastereomeric esters and separation by either crystallization or column chromatography failed, and efforts were subsequently focused on separation by chiral HPLC.

The literature contains reports of a number of studies on the resolution of AIs by chiral HPLC with particular focus on imidazole containing derivatives. Fadrozole hydrochloride was separated by Furet et al.³⁵ using a Chiralcel OD column with a hexane/2-propanol mixture as the mobile phase, and the absolute configuration of the most active enantiomer was established by an X-ray crystal structure analysis of its tartrate salt. A number of 3-methyl-6-[1-(imidazo-1-yl)-1-phenylmethyl] benzothiazolinones and 3-methyl-6-[1-(imidazo-1-yl)-1-phenylmethyl] benzoxazolinones were separated by Danel et al.³⁶ using a Chiralpak AD and a Chiralcel OD-H column, with mobile phases consisting of hexane/ethanol mixtures. The absolute configuration of these enantiomers was determined by X-ray crystal structure analysis. A series of seven triazole and imidazole containing AIs has been separated on a number of cellulose- and amylose-based chiral stationary phases by Aboul-Enein et al.,³⁷ with optimum resolution obtained with a Chiralpak AD-RH column.

Initially, the separation of the enantiomers of **39** was investigated with a range of amylose and cellulose packed columns, and the best separations obtained from this initial screen were with the Chiralpak AD-H ($\alpha = 1.55$, $R_s = 3.2$) and the Chiralpak AS-H ($\alpha = 1.3$, $R_s = 1.5$) columns with EtOH/MeOH (50:50) as the mobile phase. These conditions were further optimized to give the best separation with a Chiralpak AD-H column and MeOH as the mobile phase ($\alpha = 1.98$, $R_s = 5.11$). As shown in Figure 3, the first enantiomer was eluted from the column with a retention time of 4.76 min (**39a**), whereas the second enantiomer eluted with a retention time of 6.23 min (**39b**).

The configurational stability of a series of enantiopure imidazole containing AIs has been investigated by Danel et al.³⁸ It was reported that the enantiomeric purity of these compounds decreased following removal of the solvent on a rotary evaporator (bath temperature 40–50 $^{\circ}$ C), although this was attributed to the presence of basic impurities in the HPLC solvent. As a result of this observation, the configurational stability of **39a** was investigated by heating a solution of the compound in MeOH at 40 $^{\circ}$ C overnight. Under these conditions, the enantiomeric purity of **39a** was found³⁹ to decrease to 95.5%. As a precaution, solutions containing the separated individual enantiomers were stored in the refrigerator and evaporation of solvents was undertaken at room temperature. No racemization was detected during this study.

Suitable quantities of phenols **39a** and **39b** for sulfamoylation were obtained following successful optimization of the separation on a Chiralpak AD-H (250 mm \times 20 mm) semiprep column. The individual enantiomers obtained from the above separation were converted to their corresponding sulfamates using the previously described conditions of ClSO₂NH₂ in

DMA. To confirm that this step had not resulted in a loss of enantiomeric purity, a method was developed for the chiral HPLC separation of **40** with a Chiralpak AD-H analytical column and 85% MeOH/15% water as the mobile phase. The order of elution for the two enantiomers was found to switch following sulfamoylation, i.e., phenol **39a** with $t_r = 4.76$ min corresponds to the slower eluting sulfamate with $t_r = 12.69$ min (**40a**) and phenol **39b** with $t_r = 6.23$ min corresponds to the sulfamate with $t_r = 10.96$ min (**40b**). Although the resolution obtained for the separation of **40** was not as good as that obtained for **39**, this was satisfactory for analytical purposes. The HPLC traces of **40a** and **40b** are shown in Figure 3, and both show that there was no significant loss of enantiomeric purity during the sulfamoylation step.

The optical rotation for each enantiomer of the phenol and corresponding sulfamate was measured in an ethanolic solution. For the phenols, the rotation of **39a** is $+84.3^\circ$ ($c = 3.9$) and for **39b**, it is -79.1° ($c = 3.6$) and for the sulfamates, **40a** is $+34.2^\circ$ ($c = 0.97$) and **40b** is -30.7° ($c = 0.95$).

Determination of Absolute Configuration. Following isolation of the separated enantiomers of **39** by semiprep chiral HPLC, it was essential to determine the absolute configuration (AC) of each enantiomer **39a** and **39b**. Crystals suitable for X-ray crystal structure analysis could be obtained from racemic **39** following slow evaporation of the solvent from an EtOAc solution. However, when this was attempted with either of the single enantiomers, the product obtained was an oil. In an attempt to obtain a crystalline compound suitable for X-ray crystallography, a range of derivatives were prepared (including *N,N*-diphenylcarbamates and 1-naphthoates), but these compounds were also all obtained as oils. Extensive efforts to solve these problems ended in failure, and this necessitated the use of an alternative technique for the determination of AC.

The measurement of the chiroptical properties of a molecule in tandem with quantum mechanical calculations provides a powerful method for the determination of AC. The principle behind this is the determination of the vibrational circular dichroism (VCD)^{40–42} and/or the electronic circular dichroism (ECD)^{43,44} of an enantiomer experimentally and the comparison of these spectra with those predicted by density functional theory (DFT) calculations for one AC. As these are solution phase techniques, this approach has found particular application for the determination of AC for compounds, which are precluded from X-ray crystallography. The popularity of these techniques has increased in recent years, and in one example, VCD has been used to correct the AC of a molecule previously assigned by X-ray crystallography.⁴⁵ A combination of DFT calculations with VCD,⁴⁰ and TDDFT (time dependent DFT) calculations with ECD and optical rotation measurements, has been reported in a study by Stephens et al.⁴⁶ to determine the AC of a chiral oxadiazol-3-one, which exhibits myocardial calcium entry channel blocking activity. All three chiroptical techniques assigned identical ACs which were *R*-(+) and *S*-(−). Recently, and more relevantly to this work, Cavalli et al.⁴⁷ have reported the design of a new series of nonsteroidal AIs and the determination of AC by ECD and TDDFT calculations. Although ACs can be determined by the study of a single chiroptical property alone, agreement between two or more techniques clearly produces a more definitive assignment of AC. As these techniques have proved to be reliable, the AC of **39a** and **39b** was studied using VCD and ECD in conjunction with DFT and TDDFT calculations.

The experimental mid-IR VCD for **39a** and **39b** and the calculated mid-IR VCD for the *R* configuration of **39** are shown

in Figure 4. For the measured spectra, a good mirror-image condition was obtained for the two enantiomers. However, to eliminate baseline drift, the half-difference **39a**–**39b** is reported for **39a** and the half-difference **39b**–**39a** is reported for **39b**. The *R* configuration of **39** was arbitrarily chosen for the calculations of both the VCD and the ECD spectrum. After a full conformational search at PM3 level, subsequent B3LYP/6-3G* optimization in vacuo was performed using Gaussian 03,⁴⁸ and this gave eight conformers with energy values remarkably lower than all the others. The conformations were verified to be real energy minima, and the free energy value of each conformation was calculated in order to evaluate the relative population of each conformation at room temperature using Boltzmann statistics. The calculated spectrum⁴⁰ was obtained from the weighted average of each of the eight conformations (data not shown and will be published elsewhere). The calculated VCD spectrum for the *R* configuration corresponds well to the VCD spectra obtained for **39a**. Therefore, VCD permits the unambiguous assignment of the absolute configuration of **39a** as *R*-(+) and **39b** as *S*-(−).

The ECD measurement for each enantiomer of **39** along with that simulated by TDDFT calculations is shown in Figure 5. The spectra were obtained from methanolic solutions at concentrations of 10^{-4} M or 10^{-3} M and the spectra are solvent subtracted. The ECD spectrum of the enantiomer of **39** with the *R* configuration was calculated with a TDDFT approach; at the same functional and basis set level, rotational strength in the velocity representation have been calculated and averaged over the same conformations and populations employed for VCD.

The ECD spectrum is quite rich in bands and is reproduced quite well by the simulated spectrum despite the fact that the level of calculus is not very high and only pure electronic transitions in vacuo have been considered. In this case, the data obtained from the ECD study are sufficient to determine the AC and once again there is good correlation between the ECD spectra for **39a** and that calculated for the *R* configuration, confirming the results obtained from the VCD study.

As mentioned previously, the sulfamoylation step proceeded without loss of enantiomeric purity, allowing the AC of **40a** and **40b** to be assigned as *R*-(+) and *S*-(−) respectively.

Biological Results and Discussion

Sulfamates. The in vitro inhibition of aromatase and STS activity by each sulfamate was measured in a preparation of an intact monolayer of JEG-3 cells. The results are reported either as IC₅₀ values or as a percentage of aromatase/STS inhibition at 10 μM (Table 1). The biological activity of 4,4'-bis-sulfamate **3** was reported previously.²³

The relocation of the two sulfamate groups from the *para*-positions in **3** to the *meta*-positions in **7** gives a 30-fold increase in aromatase inhibition (IC₅₀ AROM = 3044 vs 99 nM). This resembles the phenomenon previously observed in the YM511-based DASI series²² and strongly suggests that a sulfamate group positioned at the *meta*-position of the phenyl ring of a DASI is better tolerated by the aromatase enzyme than a corresponding *para*-sulfamate. Both **3** and **7** are weak STS inhibitors, and no clear difference in their inhibitory activities can be obtained from the results obtained here. This is in contrast to the finding of the benzophenone-based series of STS inhibitors where the difference in IC₅₀ values for 4,4'-benzophenone bis-sulfamate (**2**, Figure 2) and its 3,3'-bis-sulfamate congener against recombinant human steroid sulfatase is much more prominent at 0.19 and 3.2 μM, respectively.²⁸ These results clearly

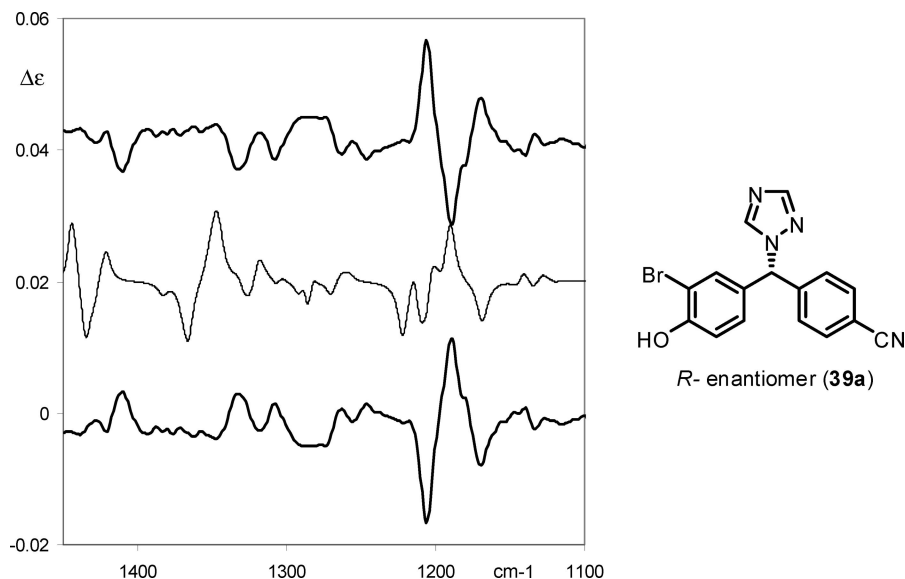


Figure 4. VCD spectra. Bottom trace: experimental spectrum of **39a** (0.256 M CDCl_3). Middle trace: calculated spectrum for *R* configuration (weighted average taking into account populations obtained by calculated Gibbs free energies). Upper trace: experimental spectrum of **39b** (0.23 M CDCl_3). Calculated frequencies have been shifted by 30 cm^{-1} .

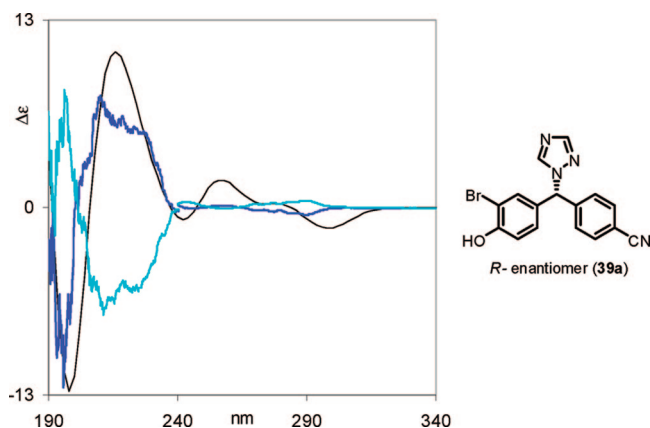


Figure 5. ECD spectra. Dark-blue trace: experimental spectrum of **39a**. Light-blue trace: experimental spectrum of compound **39b**. Black trace: calculated spectrum for *R* configuration (average over eight conformers with calculated population). The spectra were recorded on 10^{-4} M solutions in the range 190–240 nm, and on 10^{-3} M solutions in the range 240–340 nm.

demonstrate the important role played by the carbonyl group in **2** in increasing the STS inhibitory activity compared to the two triazole derivatives **3** and **7**. The carbonyl group increases the leaving group potential of the corresponding phenol, thus increasing the “sulfamoylation potential” of the aryl sulfamate and facilitating the irreversible inactivation of STS by protein sulfamoylation. This effect is expected to be strongest, with the carbonyl group *para*- to the sulfamate group explaining why **2** is a much stronger STS inhibitor than the 3,3'-bis-sulfamate derivative. For **3** and **7**, the absence of a similar electron-withdrawing group positioned *para*- to the sulfamate group contributes toward the weak STS inhibitory activities observed for these two compounds. However, based on past observations, the introduction of appropriate substituents onto the aromatic ring to increase the “sulfamoylation potential” should increase the potency of the DASIs in this series against STS.

Results published by Jones et al.⁴⁹ demonstrated that a diaryl imidazolemethane substituted with bis-methoxy groups at the *para*-position of the phenyl rings is 10-fold more active than the unsubstituted parent compound in the inhibition of aromatase

Table 1. In Vitro Inhibition of the Aromatase and STS Activity in JEG-3 Cells by Novel Sulfamates

	R ¹	R ²	R ³	R ⁴	aromatase IC ₅₀ (nM)	STS IC ₅₀ (nM)
letrozole					0.89 ± 0.13	
STX64					300 ± 42	1.5 ± 0.3
3	H	X	X	H	3044 ± 48	> 10 000
7	X	H	H	X	99 ± 0.01	31.4% @ 10 μM
10	Br	X	X	Br	43 ± 3.2	476 ± 36
16	X	OMe	OMe	X	40% @ 10 μM	10.9% @ 10 μM
22	OMe	X	X	OMe	33% @ 10 μM	11.9% @ 10 μM
28	H	X	CN	H	13 ± 4	21.5% @ 10 μM
34	Cl	X	CN	H	12 ± 3.4	920 ± 20
40	Br	X	CN	H	3.0 ± 0.1	2600 ± 100
40a R-(+)	Br	X	CN	H	3.2 ± 0.3	4633 ± 551
40b S-(-)	Br	X	CN	H	14.3 ± 2.1	553 ± 50

in vitro. This prompted us to investigate if introduction of methoxy groups to **7** would further improve the potency of aromatase inhibition. Hence, **16** was prepared but, as shown in Table 1, the ability of this compound to inhibit aromatase in JEG-3 cells was substantially reduced, giving an IC₅₀ value of > 10 μM. The exchange in position of the methoxy and sulfamate groups in **22** failed to improve the aromatase inhibitory activity as demonstrated by the comparable IC₅₀ value of **16** to **22**. Both bis-methoxy derivatives **16** and **22** showed very weak inhibitions of STS in vitro (Table 1), suggesting that the electron-donating effect of the methoxy groups is deleterious to the STS inhibitory activity of these derivatives.

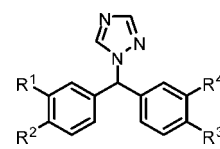
There is an increase in both aromatase and STS inhibition in the derivatives with a halogen *ortho* to the sulfamate group. Comparing **3** with **10** reveals a significant increase in potency against both enzymes, from 3044 to 43 nM for aromatase and from >10000 to 476 nM for STS. This mirrors the results obtained from our previous SAR studies on YM511-type

DASIs.^{21,22} The increase in aromatase inhibition is reasoned to be due to an increase in lipophilicity of the compound, which results in tighter binding of the halogenated derivative to the active site. The increase in STS inhibition can be attributed to a lowering of the pK_a of the phenol, enhancing its leaving group ability. This beneficial electronic effect on STS inhibition has consistently been observed in the development of steroidal STS inhibitors.^{50,51}

The introduction of two *meta*-bromo groups to give **10** improves the potency of aromatase inhibition and in addition gave the most potent STS inhibitor in this study. However, the best aromatase inhibition is obtained from a small series of monosulfamates in which more of the features of letrozole were retained. This series of compounds contains a chiral center, and these derivatives were initially synthesized and evaluated as racemic mixtures. Derivative **28** has an IC_{50} value against aromatase in JEG-3 cells of 13 nM, making it some 250-fold more potent than bis-sulfamate **3** and three times more potent than **10**. Clearly, this increase in potency against aromatase can be attributed to the presence of a *para*-cyanophenyl moiety in the molecule, which contributes significantly to the binding of the inhibitor to the enzyme active site possibly in a similar manner to letrozole. The importance of the positioning of an H-bond accepting group relative to the triazole/imidazole ring has been extensively discussed in the literature,^{52,53} and it has been postulated by Furet et al.³⁵ that in (*S*)-fadrozole the CN group acts as an H-bond acceptor in a similar manner to the steroidal 17-carbonyl group. Compared with **28**, *meta*-chloro derivative **34** is surprisingly not a stronger AI given the role that a halogen plays in the improvement of aromatase inhibition for this class of compound. However, the bromo derivative **40** exhibits a substantial improvement in aromatase inhibitory activity compared to its chloro congener **34** ($IC_{50\text{ AROM}} = 3.0$ vs 12 nM). This is a trend reflected in our finding that the *meta*-chloro derivative of **1**, a YM511-based DASI (Figure 2, R = Cl), is 3-fold weaker as an AI than its bromo-congener (**1**, Figure 2, R = Br).²¹ This increase in inhibitory activity may be caused by the increase in lipophilicity for the halogenated derivatives, which results in enhanced binding to the active site of the enzyme. In the current series, the *meta*-bromo derivative **40** is a weaker STS inhibitor than **34** ($IC_{50\text{ STS}} = 920$ nM vs 2600 nM). This effect could possibly be caused by the increased steric bulk of the bromine atom, which results in interference of the binding of this derivative in the enzyme active site.

To determine the difference in aromatase and STS inhibition for each enantiomer of **40**, the preceding phenols were separated by chiral HPLC (details given above) and converted to their corresponding sulfamates. Previous studies have suggested that there is often a large difference in aromatase inhibition between the enantiomers of chiral AIs. For fadrozole hydrochloride,³⁵ there is a 210-fold difference in aromatase inhibitory activity between enantiomers, with the *S* enantiomer proving to be the most active (*S*-form IC_{50} 3.2 nM vs *R*-form IC_{50} 680 nM). Moreover, for vorozole,⁵⁴ there is a 32-fold difference in activity, with the *R* configuration being the most active (*R*-(+)) IC_{50} 1.38 nM, *S*-(-) IC_{50} 44.2 nM and exhibiting a similar inhibition to the racemate (*RS*-(\pm)) IC_{50} 2.59 nM). Of the two enantiomers in the current study, **40a** (*R*-(+)) is more potent against aromatase while **40b** (*S*-(-)) is more potent against sulfatase. The more modest 4-fold difference in aromatase inhibition observed for **40a** ($IC_{50\text{ AROM}} = 3.2$ nM) and **40b** ($IC_{50\text{ AROM}} = 14.3$ nM) could be due to the presence of the sulfamate groups, resulting in these compounds not being optimized for aromatase inhibition. For the inhibition of aromatase, the racemate (**40**) is

Table 2. In Vitro Inhibition of the Aromatase Activity in JEG-3 Cells by Novel Phenols



	R ¹	R ²	R ³	R ⁴	aromatase IC ₅₀ (nM)
letrozole					0.89 ± 0.13
6	OH	H	H	OH	2457 ± 132
8	H	OH	OH	H	178
9	Br	OH	OH	Br	10 ± 2.7
15	OH	OMe	OMe	OH	169 ± 50
21	OMe	OH	OH	OMe	215 ± 16
27	H	OH	CN	H	7.2 ± 1.1
33	Cl	OH	CN	H	5.5 ± 3.7
39	Br	OH	CN	H	1.8 ± 0.3
39a R (+)	Br	OH	CN	H	0.6 ± 0.1
39b S (-)	Br	OH	CN	H	3.4 ± 0.6

similar in potency to the enantiomer with *R* configuration (**40a**), a finding similar to that observed for vorozole. While for STS inhibition, the activity of the racemate roughly lies halfway between the activity of each enantiomer, the activity of **40b** ($IC_{50\text{ STS}} = 553$ nM) against STS is similar to that of **10** ($IC_{50\text{ STS}} = 476$ nM), the most potent STS inhibitor in this study. Interestingly, compounds **40a** and **40b** comprise the first enantiopure, sulfamate-based, nonsteroidal STS inhibitors to be evaluated. Here, for the first time, we have demonstrated that the enantiomers of a chiral sulfamate-containing compound inhibit STS to a different extent. This 9-fold difference in potency observed for **40a** and **40b** warrants further investigation.

Phenols. Displayed in Table 2 are the IC_{50s} for aromatase inhibition obtained for the novel phenols described in this paper, with values ranging from 0.6 to 2457 nM. The loss of the sulfamate group following irreversible inactivation of STS by a sulfamate-based DASI or for some sulfamates, through degradation on prolonged circulation in plasma, will result in the formation of the corresponding phenol. As these phenols still contain the pharmacophore for aromatase inhibition, they have the potential to act as AIs in their own right.

With the exception of **6**, all of the phenols tested in this series are better AIs than their corresponding sulfamates. This trend, which was previously observed in the YM511 series, suggests that the sulfamate group is too large for optimum binding in the aromatase active site. As previously observed, the presence of a halogen *ortho* to the sulfamate group results in an increase in aromatase inhibition and this trend is also seen with the corresponding phenols. This is particularly illustrated by the difference in aromatase inhibition between **27** ($IC_{50\text{ AROM}} = 7.2$ nM) and **39** ($IC_{50\text{ AROM}} = 1.8$ nM) and is also seen for **8** ($IC_{50\text{ AROM}} = 178$ nM) and **9** ($IC_{50\text{ AROM}} = 10$ nM). Introduction of methoxy groups to **8** to give **21** failed to give the expected beneficial effects in aromatase inhibition ($IC_{50\text{ AROM}} = 178$ nM vs 215 nM), although **15** is a better AI than **6** ($IC_{50\text{ AROM}} = 169$ nM vs 2457 nM).

The best AI among the achiral and racemic compounds is phenol **39** ($IC_{50\text{ AROM}} = 1.8$ nM), while the corresponding sulfamate, **40** ($IC_{50\text{ AROM}} = 3.0$ nM), is the best AI in the same category for the sulfamate series. However, of the two enantiomers of **39**, the *R* configuration (**39a**) is not only nearly 6-fold more active than the *S* configuration (**39b**), but is also the most potent AI discovered herein, with an IC_{50} of 0.6 nM, comparable to that of letrozole. The same trend in activity is observed with

the corresponding sulfamates where the compound with the *R* configuration is the more active, in this case by around 4-fold (Table 1).

Molecular Modeling. A molecular modeling study was instigated in an attempt to investigate the difference in inhibitory activities between **39a** and **39b** for aromatase inhibition and between **40a** and **40b** for both aromatase and sulfatase inhibition. Each of the four compounds and letrozole were individually docked into the human aromatase homology model⁵⁵ using GOLD.⁵⁶ Compound **39a** was found to dock in two modes, which differed by rotation of the bromine substituted aromatic ring by $\sim 180^\circ$, and each of these modes resembled the fittest solution of letrozole (rmsd over equivalent atoms of the fittest **39a** and letrozole solutions = 0.22 Å). There was only one docking mode for **39b** in which the two phenyl rings were transposed compared to **39a**. The docking studies suggest different binding modes for **39a** and **39b**, with the important benzonitrile group positioned in different positions in the active site. Compound **40a** docked into aromatase in the same mode as **39a** and the docking of **40b** was similar to that of **39b** with the sulfamate group positioned on the opposite side of the active site to **40a**. These results suggest that there is adequate room for the sulfamoylated compounds to bind to the active site in the same mode as the equivalent phenols.

From the docking of **40a** and **40b** into the crystal structure of STS,⁵⁷ it was observed that compound **40a** docked in two modes, both of which placed the sulfamate group satisfactorily. Compound **40b** had one major binding mode, which places the groups in similar positions to those observed with **40a**. Both enantiomers docked into the same region of the active site as that occupied by STX64 with their sulfamate groups directed toward the Ca^{2+} ion and the catalytically important formylglycine residue. Given the well-established difficulties in correlating in silico binding models using scoring functions with real biological activity,⁵⁸ we have not attempted a detailed rationalization of our rather limited set of compounds.

Conclusions

A number of sulfamate containing compounds structurally related to letrozole and their precursor phenols were synthesized and tested for aromatase inhibition and dual inhibition of aromatase and STS in JEG-3 cells. The aromatase inhibition of their corresponding phenolic precursors was also determined. To achieve dual inhibition, both the pharmacophore for aromatase inhibition (a *N*-containing heterocyclic ring) and that for STS inhibition (a phenol sulfamate ester) were incorporated into a single molecule.

Comparison of the bis-sulfamates tested in this work reveals that switching the position of the sulfamate groups from the *para*- to the *meta*-positions gave better aromatase inhibition but no improvement in STS inhibition; however, the best inhibition of aromatase and STS in this subseries is achieved with bis-bromo bis-sulfamate **10** ($\text{IC}_{50 \text{ STS}} = 476 \text{ nM}$), which is the best STS inhibitor discovered in the letrozole-based DASI series. The two methoxy-containing derivatives are both weak inhibitors of both aromatase and STS. Better aromatase inhibition is obtained from the monosulfamates, which contain more of the features of letrozole, and the inhibition of both enzymes could be further enhanced by the presence of a halogen *ortho* to the sulfamate. The best AI of the achiral and racemic sulfamoylated compounds is **40** with an IC_{50} value of 3 nM. Compound **39**, the corresponding phenolic precursor to **40**, is the best AI of the phenolic achiral and racemic compounds ($\text{IC}_{50 \text{ AROM}} = 1.8 \text{ nM}$). The enantiomers of **39** were separated by chiral HPLC

and their AC was determined using VCD and ECD in conjunction with TDDFT calculations of their predicted properties. This allowed the AC of **39a** to be assigned as *R* and that of **39b** to be assigned as *S*. Each of the enantiomers was converted to its corresponding sulfamate, **40a** and **40b**, respectively, without loss of enantiopurity. Of the two enantiomers, **40a** is the better AI and **40b** is the better STS inhibitor, and in this assay, **39a** ($\text{IC}_{50 \text{ AROM}} = 0.6 \text{ nM}$) is similar in potency to letrozole ($\text{IC}_{50 \text{ AROM}} = 0.89 \text{ nM}$). Compounds **40a** and **40b** are the first enantiopure nonsteroidal STS inhibitors to undergo biological evaluation.

The phenolic precursors of the sulfamates still possess the pharmacophore for aromatase inhibition and will be formed in vivo from the sulfamate ester, following either compound degradation or inactivation of STS. In general, the phenols are better inhibitors than their respective sulfamates and there is a good correlation between the activity of the phenols and their corresponding sulfamates.

These results illustrate the feasibility of designing a letrozole-based DASI and provide a basis for development of compounds with potential for the treatment of HDBC. Furthermore, this work demonstrates the growing utility of chiroptical techniques for determination of absolute configuration.

Experimental Section

General Methods for Synthesis. All chemicals were purchased from either Aldrich Chemical Co. (Gillingham, UK) or Alfa Aesar (Heysham, UK). All organic solvents of AR grade were supplied by Fisher Scientific (Loughborough, UK). Anhydrous *N,N*-dimethylformamide (DMF), *N,N*-dimethylacetamide (DMA), and tetrahydrofuran (THF) were purchased from Aldrich. Sulfamoyl chloride was prepared by an adaptation of the method of Appel and Berger⁵⁹ and was stored as a solution under N_2 in toluene as described by Woo et al.⁶⁰

Thin layer chromatography (TLC) was performed on precoated aluminum plates (Merck, silica gel 60 F₂₅₄). Product spots were visualized either by UV irradiation at 254 nm or by staining with either alkaline potassium permanganate solution or 5% w/v dodecamolybdophosphoric acid in ethanol, followed by heating. Flash column chromatography was performed on silica gel (Davisil silica 60A) or using prepacked columns (Isolute) and gradient elution (solvents indicated in text) on the Flashmaster II system (Biotage). ¹H and ¹³C NMR spectra were recorded with either a Jeol Delta 270 MHz or a Varian Mercury VX 400 MHz spectrometer. Chemical shifts are reported in parts per million (ppm, δ) relative to tetramethylsilane (TMS) as an internal standard. Coupling constants, *J*, are recorded to the nearest 0.1 Hz. Mass spectra were recorded at the Mass Spectrometry Service Center, University of Bath. FAB mass spectra were carried out using *m*-nitrobenzyl alcohol as the matrix. Elemental analyses were performed by the Microanalysis Service, University of Bath. Melting points were determined using either a Stuart Scientific SMP3 or a Stanford Research Systems Optimelt MPA100 and are uncorrected. Optical rotations were measured with a machine supplied by Optical Activity Ltd. with 5 cm cells.

HPLC. LC/MS was performed using a Waters 2790 machine with a ZQ MicroMass spectrometer and PDA detector. The ionization technique used was either APCI or ES (as indicated in the text). A Waters "Symmetry" C18 (packing: 3.5 μm), 4.6 mm \times 100 mm column and gradient elution (flow rate) 5:95 MeCN/H₂O (0.5 mL/min) to 95:5 MeCN/H₂O (1 mL/min) over 10 min were used. HPLC was undertaken using a Waters 717 machine with Autosampler and PDA detector. The column used was a Waters "Symmetry" C18 (packing: 3.5 μm), 4.6 mm \times 150 mm with an isocratic mobile phase consisting of MeOH/H₂O (as indicated) with a flow rate of 1.4 mL/min. Analytical chiral HPLC was performed with a Chiralpak AD-H column (250 mm \times 4.6 mm, 5 μm) with methanol as the mobile phase, a flow rate of 1.0 mL/min, and a PDA detector. Semipreparative HPLC was performed with a Waters

2525 binary gradient module and a Chiralpak AD-H (250 mm × 20 mm) semiprep column with MeOH as the mobile phase at a flow rate of 18 mL/min, injecting 1.5–2.0 mL of a 10 mg/mL solution and a run time of 7 min.

VCD and ECD Measurements. VCD measurements were conducted with a JASCO FVS4000 apparatus equipped with a MCT detector, using a BaF₂ cell of 50 μm path length and 4 cm⁻¹ resolution. Measurements were taken on CDCl₃ solutions. ECD spectra were obtained at room temperature on a JASCO 500 spectropolarimeter, flushed with dry nitrogen using 0.1 cm and 1 cm quartz cuvettes adopting the following conditions: 100 nm/min scanning rate, 2 nm resolution and 32 scans. Samples were dissolved in methanol at 10⁻⁴ M or 10⁻³ M concentrations, and spectra were solvent subtracted.

General Method A: Condensation of Carbinols with Triazole. The substrate, 1,2,4-triazole and *para*-toluenesulfonic acid (*p*-TSA), dissolved/suspended in toluene were heated at reflux with a Dean–Stark separator for 24 h. The reaction mixture was allowed to cool, and the solvent was removed in vacuo.

General Method B: Hydrogenation. Pd/C (10%) was added to a solution of the substrate in THF/MeOH. The solution was stirred under an atmosphere of H₂ (provided by addition from a balloon) overnight. The excess H₂ was removed and the reaction mixture was filtered through celite with additional THF and MeOH, then the solvent was removed in vacuo.

General Method C: Sulfamoylation. A solution of sulfamoyl chloride (H₂NSO₂Cl) in toluene (0.7 M) was concentrated in vacuo at 30 °C to furnish a yellow oil, which solidified upon cooling in an ice bath. DMA and the substrate were subsequently added, and the mixture was allowed to warm to room temperature and stirred overnight.

Bis-(3-hydroxyphenyl)methanol (5). A solution of sodium borohydride (NaBH₄) (0.19 g, 5.14 mmol) in H₂O (5 mL) was added to a solution of 3,3'-dihydroxybenzophenone³⁰ **4** (1.00 g, 4.67 mmol) in EtOH (15 mL). After stirring for 1 h, the reaction mixture was added to a mixture of ice–water (40 mL) and conc HCl (2.5 mL), and the product was extracted with EtOAc (2 × 60 mL). The combined organic layers were subsequently washed with NaOH (3M, 2 × 50 mL). Following acidification of the combined basic washes, the product was extracted with EtOAc (2 × 100 mL). The combined EtOAc extracts were dried (MgSO₄), and the solvent was removed in vacuo. The crude product was purified by recrystallization from H₂O to give the title compound as a brown crystalline solid (0.86 g, 85%, mp 141–142 °C). δ_H (270 MHz, DMSO-*d*₆): 9.27 (2H, br s, ArOH), 7.05 (2H, t, *J* = 8.2, ArH), 6.84–6.72 (4H, m, ArH), 6.63–6.54 (2H, m, ArH), 5.72 (1H, br s, CHOH), 5.50 (1H, s, CHOH). LCMS (ES⁻) 215.0 ([M – H]⁻, 30%), 196.9 (10), 168.8 (15), 120.7 (100). HRMS (FAB⁺) found 216.0785, C₁₃H₁₂O₃ requires 216.0786.

1-[Bis-(3-hydroxyphenyl)methyl]-1H-[1,2,4]triazole (6). As general method A using **5** (0.75 g, 3.47 mmol), 1,2,4-triazole (0.48 g, 6.94 mmol), *p*-TSA (125 mg), and toluene (300 mL). The resulting residue was dissolved in EtOAc (75 mL), and the organic layer was washed with H₂O (3 × 75 mL), dried (MgSO₄), and the solvent was removed in vacuo. The crude product was purified by flash column chromatography (EtOAc:hexane 3:1) to give the title compound (0.82 g, 88%) as a pale-yellow oil, which formed a foam under high vacuum. δ_H (270 MHz, DMSO-*d*₆): 9.50 (2H, br s, ArOH), 8.55 (1H, s, NCHN), 8.06 (1H, s, NCHN), 7.16 (2H, t, *J* = 7.9, ArH), 6.89 (1H, s, CH), 6.75–6.68 (2H, m, ArH), 6.67–6.60 (4H, m, ArH). LRMS (FAB⁺) 268.3 ([M + H]⁺, 100%), 199.2 (85). HRMS (FAB⁺) found 268.1091, C₁₅H₁₄N₃O₂ requires 268.1086.

1-[Bis-(3-sulfamoyloxyphenyl)methyl]-1H-[1,2,4]triazole (7). As general method C using ClSO₂NH₂ (8.8 mL), DMA (7 mL), and **6** (0.30 g, 1.12 mmol). The resulting yellow solution was added to brine (30 mL), and this was extracted with EtOAc (3 × 50 mL). The organic layers were combined, washed with H₂O (3 × 50 mL), dried (MgSO₄), and the solvent was removed in vacuo. The crude product was purified by flash column chromatography (CHCl₃: acetone 1:1) to give the title compound (0.42 g, 88%) as a pale-yellow oil, which formed a foam under high vacuum. δ_H (270 MHz,

DMSO-*d*₆): 8.64 (1H, s, NCHN), 8.11 (1H, s, NCHN), 8.04 (4H, br s, 2 × NH₂), 7.49 (2H, t, *J* = 7.9, ArH), 7.36–7.16 (7H, m, ArH and CH). LRMS (FAB⁺) 426.0 ([M + H]⁺, 100%), 357.0 (50), 85.1 (50). HRMS (FAB⁺) found 426.0540, C₁₅H₁₆N₃O₆S₂ requires 426.0542.

1-[Bis-(3-bromo-4-hydroxyphenyl)methyl]-1H-[1,2,4]triazole (9). A solution of benzyltrimethylammonium tribromide (1.46 g, 3.74 mmol) in CH₂Cl₂/MeOH 1:1 (10 mL) was added dropwise over 45 min to a cooled (–78 °C) solution of 1-[bis-(4-hydroxyphenyl)methyl]-1H-[1,2,4]triazole²³ **8** (0.50 g, 1.87 mmol) in CH₂Cl₂/MeOH 1:1 (40 mL). The mixture was allowed to warm to 0 °C and stirred for 7 h and then stirred at room temperature overnight. The solvent was removed in vacuo, and the residue was dissolved in H₂O and EtOAc. The aqueous layer was extracted with EtOAc, and the combined organic layers were washed with brine, dried (Na₂SO₄), and the solvent was removed in vacuo. The crude product was purified by flash column chromatography (hexane/EtOAc 2:1) to give the title compound as a white solid (0.57 g, 72%, mp 198–205 °C). A small sample was purified by semipreparative HPLC (MeOH/H₂O, 60:40) *t*_R = 5.5 min. δ_H (400 MHz, DMSO-*d*₆): 10.45 (2H, br s, 2 × OH), 8.56 (1H, s, NCHN), 8.06 (1H, s, NCHN), 7.30 (2H, d, *J* = 2.1, ArH), 7.03 (2H, dd, *J* = 8.6, 2.1, ArH), 6.93 (2H, d, *J* = 8.6, ArH), 6.90 (1H, s CH). LCMS (APCI⁺) 425.9 ([M + H]⁺, 4%), 356.9 (100). Anal. (C₁₅H₁₁N₃O₂Br₂) C, H, N.

1-[Bis-(3-bromo-4-sulfamoyloxyphenyl)methyl]-1H-[1,2,4]triazole (10). As general method C using ClSO₂NH₂ (2.6 mL), DMA (2.5 mL), and **9** (0.18 g, 0.41 mmol). The resulting solution was added to brine (20 mL) and this was extracted with EtOAc (3 × 20 mL). The organic layers were combined, washed with H₂O (3 × 40 mL), dried (MgSO₄), and the solvent removed in vacuo. The title compound was obtained as a white solid (0.21 g, 88%, mp 98–102 °C). δ_H (270 MHz, DMSO-*d*₆): 8.69 (1H, s, NCHN), 8.32 (4H, br s, 2 × NH₂), 8.15 (1H, s, NCHN), 7.66 (2H, d, *J* = 2.2, ArH), 7.55 (2H, d, *J* = 8.4, ArH), 7.38 (2H, dd, *J* = 8.4, 2.2, ArH), 7.21 (1H, s CH). LRMS (FAB⁺) 584.0 ([M + H]⁺, 10%), 515.0 (10), 391.2 (100). HRMS (FAB⁺) found 581.8759, C₁₅H₁₄N₃O₆S₂Br₂ requires 581.8752.

Bis-(3-benzyloxy-4-methoxyphenyl)methanol (13). *n*-BuLi (1.6 M, 5.2 mL) was added slowly to a cooled (–78 °C) solution of **12** (2.10 g, 7.2 mmol) in THF (28 mL). After stirring for 1 h, a solution of 3-benzyloxy-4-methoxybenzaldehyde (1.74 g, 7.2 mmol) in THF (16 mL) was added dropwise, and the reaction mixture was stirred for 1.5 h. The reaction mixture was allowed to warm to room temperature, and after stirring for 2 h, it was quenched by the addition of H₂O (100 mL). The product was extracted with EtOAc (3 × 100 mL) and the combined organics were dried (MgSO₄) and the solvent was removed in vacuo. The crude product was purified by precipitation from EtOAc/hexane to give the title compound (1.70 g, 52%, mp 103–105 °C) as a white solid. δ_H (270 MHz, CDCl₃): 7.42–7.21 (10H, m, ArH), 6.89–6.79 (6H, m, ArH), 5.63 (1H, d, *J* = 3.5, CH), 5.06 (4H, s, 2 × CH₂), 3.86 (6H, s, 2 × CH₃), 2.02 (1H, d, *J* = 3.5, OH). LRMS (FAB⁺) 456.1 (M⁺, 45%), 439.1 (85), 349.2 (10), 243.1 (20), 91.1 (100). HRMS (FAB⁺) found 456.1944, C₂₉H₂₈O₅ requires 456.1937.

1-[Bis-(3-benzyloxy-4-methoxyphenyl)methyl]-1H-[1,2,4]triazole (14). As general method A using **13** (1.60 g, 3.50 mmol), 1,2,4-triazole (0.48 g, 6.95 mmol), *p*-TSA (160 mg), and toluene (230 mL). The resulting residue was dissolved in EtOAc (100 mL), and the organic layer was washed with H₂O (3 × 100 mL), dried (MgSO₄), and the solvent was removed in vacuo. The crude product was purified using Flashmaster II (EtOAc/hexane) to give the title compound (1.51 g, 84%, mp 96–99 °C) as a yellow oil, which solidified after standing. δ_H (400 MHz, CDCl₃): 7.95 (1H, s, NCHN), 7.67 (1H, s, NCHN), 7.34–7.24 (10H, m, ArH), 6.81 (2H, d, *J* = 8.4, ArH), 6.58–6.48 (5H, m, ArH), 5.00 (4H, s, 2 × CH₂), 3.84 (6H, s, 2 × CH₃). LRMS (FAB⁺) 507.2 (M⁺, 20%), 439.2 (100), 349.2 (15), 257.2 (15), 91.1 (35). HRMS (FAB⁺) found 507.2159, C₃₁H₂₉N₃O₄ requires 507.2158. Anal. (C₃₁H₂₉N₃O₄) C, H, N.

1-[Bis-(3-hydroxy-4-methoxyphenyl)methyl]-1H-[1,2,4]triazole (15). As general method B using Pd/C (80 mg), **14** (1.65 g, 3.25 mmol), and THF/MeOH (1:1, 200 mL). The crude product was purified using Flashmaster II (EtOAc/hexane) to give the title compound (0.86 g, 81%, mp 217.5–219 °C) as a white solid. δ_{H} (270 MHz, DMSO- d_6): 9.08 (2H, s, 2 × OH), 8.47 (1H, s, NCHN), 8.03 (1H, s, NCHN), 6.88 (2H, d, $J = 8.4$, ArH), 6.76 (1H, s, CH), 6.64 (2H, s, ArH), 6.57 (2H, d, $J = 8.4$, ArH), 3.74 (6H, s, 2 × CH₃). LCMS (ES⁻) 326.2 ([M - H]⁻, 100%), 255.9 (70), 240.4 (60), 211.4 (70). HRMS (FAB⁺) found 327.1226, C₁₇H₁₇N₃O₄ requires 327.1219. Anal. (C₁₇H₁₇N₃O₄) C, H, N.

1-[Bis-(3-sulfamoyloxy-4-methoxyphenyl)methyl]-1H-[1,2,4]triazole (16). As general method C using ClSO₂NH₂ (5.8 mL), DMA (6 mL), and **15** (0.30 g, 0.92 mmol). The resulting mixture was poured onto brine (50 mL), and this was extracted with EtOAc (3 × 50 mL). The organic layers were combined, washed with H₂O (2 × 50 mL) and brine (2 × 50 mL), dried (MgSO₄), and the solvent was removed in vacuo. The crude product was purified using Flashmaster II (EtOAc/hexane) to give the title compound (0.40 g, 90%) as a white foam. δ_{H} (270 MHz, DMSO- d_6): 8.56 (1H, s, NCHN), 8.07 (1H, s, NCHN), 7.93 (4H, br s, 2 × NH₂), 7.26–7.07 (6H, m, ArH), 7.00 (1H, s, CH), 3.80 (6H, s, 2 × CH₃). LRMS (FAB⁺) 486.1 ([M + H]⁺, 20%), 417.0 (100), 338.1 (14), 257.1 (6). HRMS (FAB⁺) found 485.0659, C₁₇H₁₉N₅O₈S₂ requires 485.0675.

1-[Bis-(4-hydroxy-3-methoxyphenyl)methyl]-1H-[1,2,4]triazole (21). As general method B using Pd/C (55 mg), **20** (1.70 g, 3.35 mmol), and THF/MeOH (1:1, 200 mL). The crude product was purified using Flashmaster II (EtOAc/Hexane) to give the title compound (0.73 g, 67%, mp 159 °C dec) as a cream solid. δ_{H} (270 MHz, DMSO- d_6): 9.12 (2H, s, 2 × OH), 8.44 (1H, s, NCHN), 8.02 (1H, s, NCHN), 6.82–6.70 (5H, m, ArH), 6.59 (2H, dd, $J = 8.2$, 2.0, ArH), 3.68 (6H, s, 2 × CH₃). LCMS (ES⁻) 326.3 ([M - H]⁻, 50%), 256.5 (50), 240.4 (100), 211.2 (20). HRMS (FAB⁺) found 327.1218, C₁₇H₁₇N₃O₄ requires 327.1219. Anal. (C₁₇H₁₇N₃O₄) C, H, N.

1-[Bis-(4-sulfamoyloxy-3-methoxyphenyl)methyl]-1H-[1,2,4]triazole (22). As general method C using ClSO₂NH₂ (5.8 mL), DMA (6 mL), and **21** (0.30 g, 0.92 mmol). The resulting reaction mixture was poured onto brine (50 mL), and this was extracted with EtOAc (3 × 50 mL). The organic layers were combined, washed with H₂O (2 × 50 mL) and brine (2 × 50 mL), dried (MgSO₄), and the solvent was removed in vacuo. The crude product was purified using Flashmaster II (EtOAc/hexane) to give the title compound (0.41 g, 93%) as a white foam. δ_{H} (270 MHz, DMSO- d_6): 8.60 (1H, s, NCHN), 8.11 (1H, s, NCHN), 7.95 (4H, br s, 2 × NH₂), 7.31 (2H, d, $J = 8.4$, ArH), 7.13 (2H, d, $J = 2.0$, ArH), 7.07 (1H, s, CH), 6.90 (2H, dd, $J = 8.4$, 2.0, ArH), 3.75 (6H, s, 2 × CH₃). LRMS (FAB⁺) 485.9 [M + H]⁺, 20%), 416.9 (35), 338.0 (10). HRMS (FAB⁺) found 485.0683, C₁₇H₁₉N₅O₈S₂ requires 485.0675.

(R,S)-1-[(4-Cyanophenyl)(4-hydroxyphenyl)methyl]-1H-[1,2,4]triazole (27). As general method A using **26** (0.20 g, 0.89 mmol), 1,2,4-triazole (0.13 g, 1.88 mmol), *p*-TSA (50 mg), and toluene (70 mL). The resulting residue was dissolved in EtOAc (20 mL) and the organic layer was washed with H₂O (3 × 40 mL) and brine (40 mL), then dried (MgSO₄), and the solvent was removed in vacuo. The crude product was purified using Flashmaster II (EtOAc/hexane) to give the title compound (0.21 g, 81%) as a white solid. δ_{H} (270 MHz, DMSO- d_6): 9.64 (1H, br s, OH), 8.56 (1H, s, NCHN), 8.08 (1H, s, NCHN), 7.84 (2H, AA'BB', ArH), 7.32 (2H, AA'BB', ArH), 7.10 (2H, AA'BB', ArH), 7.08 (1H, s, CH), 6.76 (2H, AA'BB', ArH); LRMS (FAB⁺) 277.1 ([M + H]⁺, 55%), 208.1 (100). HRMS (FAB⁺) found 277.1095, C₁₆H₁₃N₄O requires 277.1089. Anal. (C₁₆H₁₂N₄O) C, H, N.

1-[(4-Cyanophenyl)(4-sulfamoyloxyphenyl)methyl]-1H-[1,2,4]triazole (28). As general method C using ClSO₂NH₂ (5.8 mL), DMA (6 mL), and **27** (0.30 g, 0.92 mmol). The resulting reaction mixture was poured onto brine (50 mL), and this was extracted with EtOAc (3 × 50 mL). The organic layers were combined, washed with H₂O (2 × 50 mL) and brine (2 × 50 mL), dried (MgSO₄), and the solvent was removed in vacuo. The crude

product was purified using Flashmaster II (EtOAc/hexane) to give the title compound (0.42 g, 81%) as a white powder. δ_{H} (270 MHz, DMSO- d_6): 8.68 (1H, s, NCHN), 8.08 (1H, s, NCHN), 8.05 (2H, br s, NH₂), 7.88 (2H, AA'BB', ArH), 7.44–7.28 (7H, m, 6 × ArH, CH). LCMS (ES⁺) 356.0 ([M + H]⁺, 10%), 286.8 (100), 207.7 (90), 157.6 (30), 140.6 (35). HRMS (FAB⁺) found 356.0806, C₁₆H₁₄N₅O₃S requires 356.0817.

1-[(4-Cyanophenyl)(3-chloro-4-hydroxyphenyl)methyl]-1H-[1,2,4]triazole (33). As general method A using **32** (dissolved in min vol EtOAc) (1.53 g, 5.88 mmol), 1,2,4-triazole (4.00 g, 0.058 mol), *p*-TSA (0.30 g), and toluene (350 mL). The resulting residue was dissolved in EtOAc (70 mL), and the organic layer was washed with H₂O (4 × 70 mL) and brine (70 mL), then dried (MgSO₄), and the solvent was removed in vacuo. The crude product was purified using Flashmaster II (EtOAc/hexane) to give the title compound (1.24 g, 68%, mp 166.5–168 °C) as a white solid; an analytical sample was obtained by recrystallization from EtOAc. δ_{H} (400 MHz, DMSO- d_6): 10.50 (1H, br s, OH), 8.60 (1H, s, NCHN), 8.12 (1H, s, NCHN), 7.57 (2H, AA'BB', ArH), 7.35 (2H, AA'BB', ArH), 7.29 (1H, d, $J = 2.1$, ArH), 7.16 (1H, s, CH), 7.10 (1H, dd, $J = 8.8$, 2.1, ArH), 6.99 (1H, d, $J = 8.8$, ArH). LCMS (APCI⁻) 309.1 ([M - H]⁻, 60%), 241.0 (100). HRMS (FAB⁺) found 311.0709, C₁₆H₁₂N₄OCl requires 311.0700.

1-[(4-Cyanophenyl)(3-chloro-4-sulfamoyloxyphenyl)methyl]-1H-[1,2,4]triazole (34). As general method C using ClSO₂NH₂ (4.8 mL), DMA (4 mL), and **33** (0.25 g, 0.81 mmol). The resulting reaction mixture was poured onto brine (20 mL), and this was extracted with EtOAc (3 × 20 mL). The organic layers were combined, washed with H₂O (3 × 30 mL) and brine (30 mL), dried (MgSO₄), and the solvent was removed in vacuo. The crude product was purified using Flashmaster II (EtOAc/hexane) to give the title compound (0.25 g, 80%) as a white solid. δ_{H} (270 MHz, DMSO- d_6): 8.71 (1H, s, NCHN), 8.33 (2H, br s, NH₂), 8.15 (1H, s, NCHN), 7.89 (2H, AA'BB', ArH), 7.53 (1H, d, $J = 2.2$, ArH), 7.52 (1H, d, $J = 8.4$, ArH), 7.41 (2H, AA'BB', ArH), 7.35 (1H, dd, $J = 8.4$, 2.2, ArH), 7.31 (1H, s, CH). LCMS (APCI⁺) 390.2 ([M + H]⁺, 100%), 311.2 (20), 242.1 (20), 241.1 (60). HRMS (FAB⁺) found, 390.0436 C₁₆H₁₃N₅O₃SCl requires 390.0428.

4-Cyano-3'-bromo-4'-methoxybenzophenone (36). Aluminum chloride (7.08 g, 53.1 mmol) was added in small portions over 15 min to a solution of 4-cyanobenzoyl chloride (8.00 g, 48.3 mmol) in *o*-bromoanisole (40 mL) After stirring for 24 h, the reaction mixture was poured onto ice–water (120 mL) and stirred for 1 h. EtOAc (100 mL) and 3 M NaOH (400 mL) were added and the layers were separated; the aqueous was further extracted with EtOAc (2 × 150 mL). The organic layers were combined, washed with brine (2 × 200 mL), and dried (MgSO₄). The solvent was removed in vacuo to give a dark-brown oil to which hexane (200 mL) was added. The white precipitate was collected and was purified by recrystallization from EtOH and then further purified (to remove debrominated material) using Flashmaster II (EtOAc/hexane) to give the title compound (4.49 g, 29%, mp 172.5–174 °C) as a white crystalline solid. δ_{H} (270 MHz, DMSO- d_6): 8.03 (2H, AA'BB', ArH), 7.95 (1H, d, $J = 1.9$, ArH), 7.83 (2H, AA'BB', ArH), 7.76 (1H, dd, $J = 8.5$, 2.2, ArH), 7.27 (1H, d, $J = 8.5$, ArH), 3.98 (3H, s, CH₃). LCMS (APCI⁺) 316.1 (M⁺, 80%), 214.0 (45), 198.2 (100). HRMS (FAB⁺) found 315.9982, C₁₅H₁₁NO₂Br requires 315.9973.

4-Cyano-3'-bromo-4'-hydroxybenzophenone (37). BBr₃ (1 M solution in DCM, 52 mL) was slowly added to a cooled (0 °C) solution of **36** (3.30 g, 10.4 mmol) in DCM (40 mL). The resulting solution was allowed to warm to room temperature and was stirred for 6 days. The reaction mixture was poured onto ice–water (200 mL) and extracted with DCM (2 × 200 mL), the combined organics were washed with H₂O (250 mL) and NaHCO₃ (250 mL) and were extracted with NaOH (3 M, 3 × 150 mL). The combined basic extracts were acidified with conc HCl and extracted with DCM (2 × 200 mL), the combined extracts were washed with H₂O (2 × 100 mL), dried, (MgSO₄) and the solvent was removed in vacuo. The title compound (2.00 g, 64%, mp 216 °C (dec)) was obtained as a cream solid. δ_{H} (270 MHz, DMSO- d_6): 11.50 (1H, br s, OH), 8.01 (2H, AA'BB', ArH), 7.88 (1H, d, $J = 1.9$, ArH) 7.81 (2H,

AA'BB', ArH), 7.62 (1H, dd, $J = 8.5, 1.9$, ArH), 7.08 (1H, d, $J = 8.5$, ArH). LCMS (APCI⁻) 302.1 (M⁻, 50%), 222.0 (100), 212.0 (25). HRMS (FAB⁺) found 301.9823, C₁₄H₉NO₂Br requires 301.9817.

(4-Cyanophenyl)(3-bromo-4-hydroxyphenyl)methanol (38). A solution of NaBH₄ (0.53 g, 13.9 mmol) in H₂O (8 mL) was added dropwise to a solution of **37** (2.00 g, 7.75 mmol) in EtOH (20 mL). After stirring overnight, the reaction mixture was added to aq HCl (3 M, 40 mL) and the product was extracted with DCM (3 × 30 mL). The combined organic layers were washed with brine (60 mL), dried (MgSO₄), and the solvent was removed in vacuo. The crude product was purified using Flashmaster II (EtOAc/hexane) to give the title compound (1.67 g, 83%) as an oil which solidified on standing to give a pink solid. δ_{H} (270 MHz, DMSO-*d*₆): 10.17 (1H, br s, OH) 7.76 (2H, AA'BB', ArH), 7.54 (2H, AA'BB', ArH), 7.44 (1H, d, $J = 2.0$, ArH), 7.13 (1H, dd, $J = 8.4, 2.0$, ArH), 6.87 (1H, d, $J = 8.4$, ArH), 6.08 (1H, d, $J = 3.9$, OH), 5.69 (1H, d, $J = 3.9$, CH). LCMS (APCI⁻) 302.2 ([M - 1]⁻, 80%), 284.2 (100). HRMS (FAB⁺) found 303.9968, C₁₄H₁₁BrNO₂ requires 303.9968.

1-[(4-Cyanophenyl)(3-bromo-4-hydroxyphenyl)methyl]-1H-[1,2,4]triazole (39). As general method A using **38** (dissolved in min vol EtOAc) (1.32 g, 4.34 mmol), 1,2,4-triazole (3.00 g, 43.4 mmol), *p*-TSA (0.26 g), and toluene (350 mL). The resulting residue was dissolved in EtOAc (70 mL) and the organic layer was washed with H₂O (4 × 70 mL) and brine (70 mL), then dried (MgSO₄), and the solvent was removed in vacuo. The crude product was purified using Flashmaster II (EtOAc/hexane) to give the title compound (0.94 g, 61%, mp 171.5–173.5 °C) as a white solid. δ_{H} (270 MHz, DMSO-*d*₆): 10.54 (1H, br s, OH), 8.62 (1H, s, NCHN), 8.09 (1H, s, NCHN), 7.84 (2H, AA'BB', ArH), 7.41 (1H, d, $J = 2.0$, ArH), 7.32 (2H, AA'BB', ArH), 7.13–7.07 (2H, m, ArH and CH), 6.94 (1H, d, $J = 8.4$, ArH). LCMS (APCI⁺) 354.8 ([M + H]⁺, 100%), 287.8 (20), 213.9 (40), 112.9 (100). HRMS (FAB⁺) found 355.0180, C₁₆H₁₂N₄OBr requires 355.0190. Anal. (C₁₆H₁₁BrN₄O) C, H, N.

1-[(4-Cyanophenyl)(3-bromo-4-sulfamoyloxyphenyl)methyl]-1H-[1,2,4]triazole (40). As general method C using ClSO₂NH₂ (4.8 mL), DMA (4 mL), and **39** (0.40 g, 1.13 mmol). The resulting reaction mixture was poured onto H₂O (25 mL), and this was extracted with EtOAc (2 × 30 mL). The organic layers were combined, washed with H₂O (4 × 30 mL) and brine (30 mL), dried (MgSO₄), and the solvent was removed in vacuo. The crude product was purified using Flashmaster II (EtOAc/hexane) to give the title compound (0.46 g, 88%) as a white solid. δ_{H} (270 MHz, DMSO-*d*₆): 8.69 (1H, s, NCHN), 8.30 (2H, br s, NH₂), 8.12 (1H, s, NCHN), 7.86 (2H, AA'BB', ArH), 7.65 (1H, d, $J = 2.2$, ArH), 7.50 (1H, d, $J = 8.2$, ArH), 7.42–7.33 (3H, m, ArH), 7.29 (1H, s, CH). LCMS (APCI⁻) 433.9 ([M - H]⁻, 100%), 354.9 (50), 284.8 (60), 211.8 (40). HRMS (FAB⁺) found, 433.9915 C₁₆H₁₃N₅O₃SBr requires 433.9922. HPLC (MeOH/H₂O, 80:20) $t_{\text{R}} = 1.75$ min (purity: 99%).

(R)-1-[(4-Cyanophenyl)(3-bromo-4-hydroxyphenyl)methyl]-1H-[1,2,4]triazole (39a). This was obtained following separation of **39** on a Chiralpak AD-H (250 × 20 mm) semiprep column as described in the text (t_1 4.76 min). $[\alpha]_{\text{D}}^{20} + 84.3^\circ$ ($c = 3.9$) in EtOH.

(S)-1-[(4-Cyanophenyl)(3-bromo-4-hydroxyphenyl)methyl]-1H-[1,2,4]triazole (39b). This was obtained following separation of **39** on a Chiralpak AD-H (250 × 20 mm) semiprep column as described in the text (t_2 6.23 min). $[\alpha]_{\text{D}}^{20} - 79.1^\circ$ ($c = 3.6$) in EtOH.

(R)-1-[(4-Cyanophenyl)(3-bromo-4-sulfamoyloxyphenyl)methyl]-1H-[1,2,4]triazole (40a). Prepared from **39a** as **40**. $[\alpha]_{\text{D}}^{20} + 34.2^\circ$ ($c = 0.97$) in EtOH.

(S)-1-[(4-Cyanophenyl)(3-bromo-4-sulfamoyloxyphenyl)methyl]-1H-[1,2,4]triazole (40b). Prepared from **39b** as **40**. $[\alpha]_{\text{D}}^{20} - 30.7^\circ$ ($c = 0.95$) in EtOH.

Molecular Modeling. Models of **39a/b**, **40a/b**, and letrozole were built in the SYBYL 7.3⁶¹ molecular modeling program. To obtain low energy conformations of these models, energy minimization was performed to convergence using the MMFF94s force field with MMFF94 charges. A homology model of the human

aromatase enzyme, which is based on the crystal structure of the human CYP2C9⁶² metabolic enzyme as described by Favia et al.,⁵⁵ was constructed using SYBYL7.3. Hydrogen atoms were built onto the model and all atoms except hydrogens were fixed in aggregates. Hydrogen atom positions were then optimized to convergence using the Tripos force field with Gasteiger–Hückel charges. The GOLD docking program V3.1.1 was used to dock the models to the aromatase model. The aromatase active site was defined as a 12 Å sphere around the heme group iron atom. A distance constraint (minimum = 2.00 Å, maximum = 2.30 Å) was applied between the ligating triazole nitrogen atom of the ligand to the heme iron atom. The coordination number of the iron atom was defined as 6. The ligands were then docked to the enzyme a total of 25 times each using the GOLDScore fitness function.

The 1P49.pdb crystal structure of human placental estrone/DHEA sulfatase was used for the building of the gem-diol form of STS.⁵⁷ This involved a point mutation of the ALS75 residue in the crystal structure to the gem-diol form of the structure using editing tools within SYBYL 7.3. The resulting structure was then minimized with the backbone atoms fixed to allow the gem-diol and surrounding side chain atoms to adopt low energy conformations. Minimisations were undertaken using SYBYL 7.3 applying the AMBER7 99 force field with Gasteiger–Hückel charges as implemented within SYBYL 7.3. To mimic the sulfamate group of E1S, all sulfamate based compounds were docked into the active site with their sulfamate group in its monoanionic form (i.e., -OSO₂NH⁻).

In Vitro and in Vivo Aromatase and Sulfatase Assays. Biological activities were performed essentially as described previously.²² The extent of in vitro inhibition of aromatase and sulfatase activities was assessed using intact monolayers of JEG-3 cells. Aromatase activity was measured using [1 β -³H] androstenedione (30 Ci/mmol, Perkin-Elmer Life Sciences, MA) over a 3 h period. Sulfatase activity was measured using [6,7-³H] E1S (50 Ci/mmol, Perkin-Elmer Life Sciences) over a 3 h period.

Acknowledgment. This work was supported by Sterix Ltd., a member of the Ipsen group. We thank A. C. Smith for technical assistance and Dr. Brian Freer of Chiral Technologies Europe for assistance with the chiral HPLC.

Supporting Information Available: Synthetic procedures for **12**, **18–20**, **25**, **26**, **30–32**, **42**, **43**; ¹³C NMR data for **5–7**, **13–16**, **21**, **22**, **27**, **28**, **33**, **34**, **36–40**; Microanalysis data for **9**, **14–15**, **21**, **26–27**, **39** and HPLC data for **6–7**, **10**, **16**, **22**, **28**, **33–34**, **40**. This material is available free of charge via the Internet at <http://pubs.acs.org>.

References

- (1) Brodie, A. Aromatase inhibitors in breast cancer. *Trends Endocrinol. Metab.* **2002**, *13*, 61–65.
- (2) Recanatini, M.; Cavalli, A.; Valenti, P. Nonsteroidal aromatase inhibitors: recent advances. *Med. Res. Rev.* **2002**, *22*, 282–304.
- (3) Smith, H. J.; Nicholls, P. J.; Simons, C.; Le Lain, R. Inhibitors of steroidogenesis as agents for the treatment of hormone-dependent cancers. *Expert Opin. Ther. Pat.* **2001**, *11*, 789–824.
- (4) Brueggemeier, R. W.; Hackett, J. C.; Diaz-Cruz, E. S. Aromatase inhibitors in the treatment of breast cancer. *Endocr. Rev.* **2005**, *26*, 331–345.
- (5) Dixon, J. M. Aromatase inhibitors in early breast cancer therapy: a variety of treatment strategies. *Expert Opin. Pharmacother.* **2006**, *7*, 2465–2479.
- (6) Howell, A.; Cuzick, J.; Baum, M.; Buzdar, A.; Dowsett, M.; Forbes, J. F.; Hochtin-Boes, G.; Houghton, I.; Locker, G. Y.; Tobias, J. S. Results of the ATAC (Arimidex, Tamoxifen, Alone or in Combination) trial after completion of 5 years' adjuvant treatment for breast cancer. *Lancet* **2005**, *365*, 60–62.
- (7) The Breast International Group (BIG) 1–98 Collaborative Group. A comparison of letrozole and tamoxifen in postmenopausal women with early breast cancer. *N. Engl. J. Med.* **2005**, *353*, 2747–2757.
- (8) Coombes, R. C.; Hall, E.; Gibson, L. J.; Paridaens, R.; Jassem, J.; Delozier, T.; Jones, S. E.; Alvarez, I.; Bertelli, G.; Ortmann, O.; Coates, A. S.; Bajetta, E.; Dodwell, D.; Coleman, R. E.; Fallowfield, L. J.; Mickiewicz, E.; Andersen, J.; Lonning, P. E.; Cocconi, G.; Stewart,

- A.; Stuart, N.; Snowdon, C. F.; Carpentieri, M.; Massimini, G.; Bliss, J. M. A randomized trial of exemestane after two to three years of tamoxifen therapy in postmenopausal women with primary breast cancer. *N. Engl. J. Med.* **2004**, *350*, 1081–1092.
- (9) Haynes, B. P.; Dowsett, M.; Miller, W. R.; Dixon, J. M.; Bhatnagar, A. S. The pharmacology of letrozole. *J. Steroid Biochem. Mol. Biol.* **2003**, *87*, 35–45.
- (10) Monnier, A. Refining the postmenopausal breast cancer treatment paradigm: the FACE trial. *Expert Rev. Anticancer Ther.* **2006**, *6*, 1355–1359.
- (11) Santner, S. J.; Feil, P. D.; Santen, R. J. In situ estrogen production via the estrone sulfatase pathway in breast tumors: relative importance versus the aromatase pathway. *J. Clin. Endocrinol. Metab.* **1984**, *59*, 29–33.
- (12) Poulin, R.; Labrie, F. Stimulation of cell proliferation and estrogenic response by adrenal C₁₉- Δ^5 -steroids in the Zr-75-1 human breast cancer cell line. *Cancer Res.* **1986**, *46*, 4933–4937.
- (13) Dauvois, S.; Labrie, F. Androstenedione and androst-5-ene-3 β ,17 β -diol stimulate DMBA-induced rat mammary tumors: role of aromatase. *Breast Cancer Res. Treat.* **1989**, *13*, 61–69.
- (14) Howarth, N. M.; Purohit, A.; Reed, M. J.; Potter, B. V. L. Estrone sulfamates: potent inhibitors of estrone sulfatase with therapeutic potential. *J. Med. Chem.* **1994**, *37*, 219–221.
- (15) Woo, L. W. L.; Howarth, N. M.; Purohit, A.; Hejaz, H. A. M.; Reed, M. J.; Potter, B. V. L. Steroidal and nonsteroidal sulfamates as potent inhibitors of steroid sulfatase. *J. Med. Chem.* **1998**, *41*, 1068–1083.
- (16) Reed, M. J.; Purohit, A.; Woo, L. W. L.; Newman, S. P.; Potter, B. V. L. Steroid sulfatase: molecular biology, regulation, and inhibition. *Endocr. Rev.* **2005**, *26*, 171–202.
- (17) Woo, L. W. L.; Purohit, A.; Malini, B.; Reed, M. J.; Potter, B. V. L. Potent active site-directed inhibition of steroid sulphatase by tricyclic coumarin-based sulphamates. *Chem. Biol.* **2000**, *7*, 773–791.
- (18) Malini, B.; Purohit, A.; Ganeshapillai, D.; Woo, L. W. L.; Potter, B. V. L.; Reed, M. J. Inhibition of steroid sulphatase activity by tricyclic coumarin sulphamates. *J. Steroid Biochem. Mol. Biol.* **2000**, *75*, 253–258.
- (19) Purohit, A.; Woo, L. W. L.; Potter, B. V. L.; Reed, M. J. In vivo inhibition of estrone sulfatase activity and growth of nitrosomethylurea-induced mammary tumors by 667 COUMATE. *Cancer Res.* **2000**, *60*, 3394–3396.
- (20) Stanway, S. J.; Purohit, A.; Woo, L. W. L.; Sufi, S.; Vigushin, D.; Ward, R.; Wilson, R. H.; Stanczyk, F. Z.; Dobbs, N.; Kulinskaya, E.; Elliott, M.; Potter, B. V. L.; Reed, M. J.; Coombes, R. C. Phase I study of STX 64 (667 Coumate) in breast cancer patients: the first study of a steroid sulfatase inhibitor. *Clin. Cancer Res.* **2006**, *12*, 1585–1592.
- (21) Woo, L. W. L.; Sutcliffe, O. B.; Bubert, C.; Grasso, A.; Chander, S. K.; Purohit, A.; Reed, M. J.; Potter, B. V. L. First dual aromatase–steroid sulfatase inhibitors. *J. Med. Chem.* **2003**, *46*, 3193–3196.
- (22) Woo, L. W. L.; Bubert, C.; Sutcliffe, O. B.; Smith, A.; Chander, S. K.; Mahon, M. F.; Purohit, A.; Reed, M. J.; Potter, B. V. L. Dual aromatase–steroid sulfatase inhibitors. *J. Med. Chem.* **2007**, *50*, 3540–3560.
- (23) Wood, P. M.; Woo, L. W. L.; Humphreys, A.; Chander, S. K.; Purohit, A.; Reed, M. J.; Potter, B. V. L. A letrozole-based dual aromatase–sulphatase inhibitor with in vivo activity. *J. Steroid Biochem. Mol. Biol.* **2005**, *94*, 123–130.
- (24) Jackson, T.; Woo, L. W. L.; Trusselle, M. N.; Chander, S. K.; Purohit, A.; Reed, M. J.; Potter, B. V. L. Dual aromatase–sulphatase inhibitors based on the anastrozole template: synthesis, in vitro SAR, molecular modelling and in vivo activity. *Org. Biomol. Chem.* **2007**, *5*, 2940–2952.
- (25) Numazawa, M.; Tominaga, T.; Watari, Y.; Tada, Y. Inhibition of estrone sulfatase by aromatase inhibitor-based estrogen 3-sulfamates. *Steroids* **2006**, *71*, 371–379.
- (26) Numazawa, M.; Ando, M.; Watari, Y.; Tominaga, T.; Hayata, Y.; Yoshimura, A. Structure–activity relationships of 2-, 4-, or 6-substituted estrogens as aromatase inhibitors. *J. Steroid Biochem. Mol. Biol.* **2005**, *96*, 51–58.
- (27) Hejaz, H. A. M.; Woo, L. W. L.; Purohit, A.; Reed, M. J.; Potter, B. V. L. Synthesis, in vitro and in vivo activity of benzophenone-based inhibitors of steroid sulfatase. *Bioorg. Med. Chem.* **2004**, *12*, 2759–2772.
- (28) Nussbaumer, P.; Bilban, M.; Billich, A. 4,4'-Benzophenone-O,O'-disulfamate: a potent inhibitor of steroid sulfatase. *Bioorg. Med. Chem. Lett.* **2002**, *12*, 2093–2095.
- (29) Bowman, R. M.; Steele, R. E.; Browne, L. U.S. Patent 4,978,672, 1990.
- (30) Wittig, G.; Gauss, W. Über die verzögerte autoxydation des benzaldehyds in gegenwart von asymm. diaryl-äthylenen. *Chem. Ber.* **1947**, *80*, 363–375.
- (31) Okada, M.; Iwashita, S.; Koizumi, N. Efficient general method for sulfamoylation of a hydroxyl group. *Tetrahedron Lett.* **2000**, *41*, 7047–7051.
- (32) Van der Mey, M.; Hatzelmann, A.; Van Klink, G. P. M.; Van der Laan, I. J.; Sterk, G. J.; Thibaut, U.; Ulrich, W. R.; Timmerman, H. Novel selective PDE4 inhibitors. 2. Synthesis and structure–activity relationships of 4-aryl-substituted *cis*-tetra- and *cis*-hexahydrophthalazinones. *J. Med. Chem.* **2001**, *44*, 2523–2535.
- (33) Leigh, W. J.; Arnold, D. R.; Humphreys, R. W. R.; Po, C. W. Merostabilization in radical ions, triplets, and biradicals. 4. Substituent effects on the half-wave reduction potentials and n,π^* triplet energies of aromatic ketones. *Can. J. Chem.* **1980**, *58*, 2537–2549.
- (34) Duplais, C.; Bures, F.; Sapountzis, I.; Korn, T. J.; Cahiez, G.; Knochel, P. An efficient synthesis of diaryl ketones by iron-catalyzed arylation of aryl cyanides. *Angew. Chem., Int. Ed.* **2004**, *43*, 2968–2970.
- (35) Furet, P.; Batzl, C.; Bhatnagar, A.; Francotte, E.; Rihs, G.; Lang, M. Aromatase inhibitors: synthesis, biological activity, and binding mode of azole-type compounds. *J. Med. Chem.* **1993**, *36*, 1393–1400.
- (36) Danel, C.; Foulon, C.; Guelzim, A.; Park, C. H.; Bonte, J. P.; Vaccher, C. Preparative enantiomeric separation of new aromatase inhibitors by HPLC on polysaccharide-based chiral stationary phases: determination of enantiomeric purity and assignment of absolute stereochemistry by X-ray structure analysis. *Chirality* **2005**, *17*, 600–607.
- (37) Aboul-Enein, H. Y.; Ali, I.; Gubitz, G.; Simons, C.; Nicholls, P. J. HPLC enantiomeric resolution of novel aromatase inhibitors on cellulose- and amylose-based chiral stationary phases under reversed phase mode. *Chirality* **2000**, *12*, 727–733.
- (38) Danel, C.; Foulon, C.; Goossens, J. F.; Bonte, J. P.; Vaccher, C. Kinetics of racemization of enantiopure *N*-imidazole derivatives, aromatase inhibitors: studies in organic, aqueous, and biomimetic media. *Tetrahedron: Asymmetry* **2006**, *17*, 2317–2321.
- (39) Chiral Technologies Europe. Personal Communication.
- (40) Stephens, P. J.; Ashvar, C. S.; Devlin, F. J.; Cheeseman, J. R.; Frisch, M. J. Ab initio calculation of atomic axial tensors and vibrational rotational strengths using density functional theory. *Mol. Phys.* **1996**, *89*, 579–594.
- (41) Freedman, T. B.; Cao, X. L.; Dukor, R. K.; Nafie, L. A. Absolute configuration determination of chiral molecules in the solution state using vibrational circular dichroism. *Chirality* **2003**, *15*, 743–758.
- (42) Polavarapu, P. L.; He, J. T. Chiral analysis using mid-IR vibrational CD spectroscopy. *Anal. Chem.* **2004**, *76*, 61A–67A.
- (43) Braun, M.; Hohmann, A.; Rahematpura, J.; Buhne, C.; Grimme, S. Synthesis and determination of the absolute configuration of fugomycin and desoxyfugomycin: CD spectroscopy and fungicidal activity of butenolides. *Chem.—Eur. J.* **2004**, *10*, 4584–4593.
- (44) Lebon, F.; Longhi, G.; Gangemi, F.; Abbate, S.; Priess, J.; Juza, M.; Bazzini, C.; Caronna, T.; Mele, A. Chiroptical properties of some monoazapentahelicenes. *J. Phys. Chem. A* **2004**, *108*, 11752–11761.
- (45) Devlin, F. J.; Stephens, P. J.; Besse, P. Are the absolute configurations of 2-(1-hydroxyethyl)-chromen-4-one and its 6-bromo derivative determined by X-ray crystallography correct? A vibrational circular dichroism study of their acetate derivatives. *Tetrahedron: Asymmetry* **2005**, *16*, 1557–1566.
- (46) Stephens, P. J.; Devlin, F. J.; Gasparrini, F.; Ciogli, A.; Spinelli, D.; Cosimelli, B. Determination of the absolute configuration of a chiral oxadiazol-3-one calcium channel blocker, resolved using chiral chromatography, via concerted density functional theory calculations of its vibrational circular dichroism, electronic circular dichroism, and optical rotation. *J. Org. Chem.* **2007**, *72*, 4707–4715.
- (47) Cavalli, A.; Bisi, A.; Bertucci, C.; Rosini, C.; Paluszczak, A.; Gobbi, S.; Giorgio, E.; Rampa, A.; Belluti, F.; Piazzini, L.; Valenti, P.; Hartmann, R. W.; Recanatini, M. Enantioselective nonsteroidal aromatase inhibitors identified through a multidisciplinary medicinal chemistry approach. *J. Med. Chem.* **2005**, *48*, 7282–7289.
- (48) Frisch, M. J.; Trucks, G. W.; Schlegel, H. B.; Scuseria, G. E.; Robb, M. A.; Cheeseman, J. R.; Montgomery, J. A., Jr.; Vreven, T.; Kudin, K. N.; Burant, J. C.; Millam, J. M.; Iyengar, S. S.; Tomasi, J.; Barone, V.; Mennucci, B.; Cossi, M.; Scalmani, G.; Rega, N.; Petersson, G. A.; Nakatsuji, H.; Hada, M.; Ehara, M.; Toyota, K.; Fukuda, R.; Hasegawa, J.; Ishida, M.; Nakajima, T.; Honda, Y.; Kitao, O.; Nakai, H.; Klene, M.; Li, X.; Knox, J. E.; Hratchian, H. P.; Cross, J. B.; Bakken, V.; Adamo, C.; Jaramillo, J.; Gomperts, R.; Stratmann, R. E.; Yazayev, O.; Austin, A. J.; Cammi, R.; Pomelli, C.; Ochterski, J. W.; Ayala, P. Y.; Morokuma, K.; Voth, G. A.; Salvador, P.; Dannenberg, J. J.; Zakrzewski, V. G.; Dapprich, S.; Daniels, A. D.; Strain, M. C.; Farkas, O.; Malick, D. K.; Rabuck, A. D.; Raghavachari, K.; Foresman, J. B.; Ortiz, J. V.; Cui, Q.; Baboul, A. G.; Clifford, S.; Cioslowski, J.; Stefanov, B. B.; Liu, G.; Liashenko, A.; Piskorz, P.; Komaromi, I.; Martin, R. L.; Fox, D. J.; Keith, T.; Al-Laham, M. A.; Peng, C. Y.; Nanayakkara, A.; Challacombe, M.; Gill, P. M. W.; Johnson, B.; Chen,

- W.; Wong, M. W.; Gonzalez, C.; Pople, J. A. *Gaussian 03*, revision C.02; Gaussian, Inc.: Wallingford, CT, 2004.
- (49) Jones, C. D.; Winter, M. A.; Hirsch, K. S.; Stamm, N.; Taylor, H. M.; Holden, H. E.; Davenport, J. D.; Vonkumkals, E. V.; Suhr, R. G. Estrogen synthetase Inhibitors. 2. Comparison of the in vitro aromatase inhibitory activity for a variety of nitrogen heterocycles substituted with diarylmethane or diarylmethanol groups. *J. Med. Chem.* **1990**, *33*, 416–429.
- (50) Purohit, A.; Vernon, K. A.; Wagenaar Hummelinck, A. E.; Woo, L. W. L.; Hejaz, H. A. M.; Potter, B. V. L.; Reed, M. J. The development of A-ring modified analogues of oestrone-3-*O*-sulphamate as potent steroid sulphatase inhibitors with reduced oestrogenicity. *J. Steroid Biochem. Mol. Biol.* **1998**, *64*, 269–275.
- (51) Reed, J. E.; Woo, L. W. L.; Robinson, J. J.; Leblond, B.; Leese, M. P.; Purohit, A.; Reed, M. J.; Potter, B. V. L. 2-Difluoromethyloestrone 3-*O*-sulphamate, a highly potent steroid sulphatase inhibitor. *Biochem. Biophys. Res. Commun.* **2004**, *317*, 169–175.
- (52) Gobbi, S.; Cavalli, A.; Negri, M.; Schewe, K. E.; Belluti, F.; Piazzini, L.; Hartmann, R. W.; Recanatini, M.; Bisi, A. Imidazolylmethylbenzophenones as highly potent aromatase Inhibitors. *J. Med. Chem.* **2007**, *50*, 3420–3422.
- (53) Recanatini, M.; Bisi, A.; Cavalli, A.; Belluti, F.; Gobbi, S.; Rampa, A.; Valenti, P.; Palzer, M.; Paluszczak, A.; Hartmann, R. W. A new class of nonsteroidal aromatase inhibitors: Design and synthesis of chromone and xanthone derivatives and inhibition of the P450 enzymes aromatase and 17 α -hydroxylase/C17,20-lyase. *J. Med. Chem.* **2001**, *44*, 672–680.
- (54) Vanden Bossche, H.; Willemsens, G.; Roels, I.; Bellens, D.; Moereels, H.; Coene, M. C.; Lejeune, L.; Lauwers, W.; Janssen, P. A. J. R 76713 and enantiomers: selective, nonsteroidal inhibitors of the cytochrome P450-dependent estrogen synthesis. *Biochem. Pharmacol.* **1990**, *40*, 1707–1718.
- (55) Favia, A. D.; Cavalli, A.; Masetti, M.; Carotti, A.; Recanatini, M. Three-dimensional model of the human aromatase enzyme and density functional parameterization of the iron-containing protoporphyrin IX for a molecular dynamics study of heme-cysteinato cytochromes. *Proteins: Struct., Funct., Bioinf.* **2006**, *62*, 1074–1087.
- (56) Jones, G.; Willett, P.; Glen, R. C.; Leach, A. R.; Taylor, R. Development and validation of a genetic algorithm for flexible docking. *J. Mol. Biol.* **1997**, *267*, 727–748.
- (57) Hernandez-Guzman, F. G.; Higashiyama, T.; Pangborn, W.; Osawa, Y.; Ghosh, D. Structure of human estrone sulfatase suggests functional roles of membrane association. *J. Biol. Chem.* **2003**, *278*, 22989–22997.
- (58) Warren, G. L.; Andrews, C. W.; Capelli, A. M.; Clarke, B.; LaLonde, J.; Lambert, M. H.; Lindvall, M.; Nevins, N.; Semus, S. F.; Senger, S.; Tedesco, G.; Wall, I. D.; Woolven, J. M.; Peishoff, C. E.; Head, M. S. A critical assessment of docking programs and scoring functions. *J. Med. Chem.* **2006**, *49*, 5912–5931.
- (59) Appel, R.; Berger, G. Hydrazinsulfonsaure-amide. 1. Über das hydrazodisulfamid. *Chem. Ber.* **1958**, 1339–1341.
- (60) Woo, L. W. L.; Lightowler, M.; Purohit, A.; Reed, M. J.; Potter, B. V. L. Heteroatom-substituted analogues of the active-site directed inhibitor estra-1,3,5(10)-trien-17-one-3-sulphamate inhibit estrone sulphatase by a different mechanism. *J. Steroid Biochem. Mol. Biol.* **1996**, *57*, 79–88.
- (61) SYBYL 7.3; Tripos Inc.: St. Louis, MO; 1699 South Hanley Road, St. Louis, Missouri, 63144.
- (62) Williams, P. A.; Cosme, J.; Ward, A.; Angova, H. C.; Vinkovic, D. M.; Jhoti, H. Crystal structure of human cytochrome P450C9 with bound warfarin. *Nature* **2003**, *424*, 464–468.

JM800168S